



OPEN ACCESS

EDITED BY

Yu Qi,
Yanshan University, China

REVIEWED BY

Mingjun Zou,
North China University of Water Resources
and Electric Power, China
Yaping Huang,
China University of Mining and
Technology, China
Xuelong Li,
Shandong University of Science and
Technology, China

*CORRESPONDENCE

Ruidong Yang,
✉ rdyang@gzu.edu.cn
Tongsheng Yi,
✉ gzsmtdzys@vip.163.com

SPECIALTY SECTION

This article was submitted to Economic
Geology,
a section of the journal
Frontiers in Earth Science

RECEIVED 28 November 2022

ACCEPTED 28 December 2022

PUBLISHED 12 January 2023

CITATION

Lv F, Yang R, Yi T, Gao W, Wang X,
Cheng W, Zhang Y, Li R, Yan Z, Liu Y and
Li G (2023), Characteristics of *in situ* stress
field of coalbed methane reservoir and its
influence on permeability in western
Guizhou coalfield, China.
Front. Earth Sci. 10:1110254.
doi: 10.3389/feart.2022.1110254

COPYRIGHT

© 2023 Lv, Yang, Yi, Gao, Wang, Cheng,
Zhang, Li, Yan, Liu and Li. This is an open-
access article distributed under the terms
of the [Creative Commons Attribution
License \(CC BY\)](https://creativecommons.org/licenses/by/4.0/). The use, distribution or
reproduction in other forums is permitted,
provided the original author(s) and the
copyright owner(s) are credited and that
the original publication in this journal is
cited, in accordance with accepted
academic practice. No use, distribution or
reproduction is permitted which does not
comply with these terms.

Characteristics of *in situ* stress field of coalbed methane reservoir and its influence on permeability in western Guizhou coalfield, China

Fang Lv^{1,2}, Ruidong Yang^{1,2*}, Tongsheng Yi^{3*}, Wei Gao^{3,4}, Xu Wang⁵, Wei Cheng⁶, Yan Zhang^{1,2}, Ronglei Li^{3,4}, Zhihua Yan^{3,4}, Yaohui Liu⁷ and Geng Li⁸

¹College of Resources and Environmental Engineering, Guizhou University, Guiyang, China, ²Key Laboratory of Karst Geological Resources and Environment, Ministry of Education, Guizhou University, Guiyang, China, ³Guizhou Coalfield Geological Bureau, Guiyang, China, ⁴Guizhou Coalbed Methane and Shale Gas Engineering Technology Research Center, Guiyang, China, ⁵School of Mathematics and Statistics, Liupanshui Normal University, Liupanshui, China, ⁶School of Mining Engineering, Guizhou University, Guiyang, China, ⁷School of Mechanics and Civil Engineering, China University of Mining and Technology, Xuzhou, China, ⁸School of Resources and Geosciences, China University of Mining and Technology, Xuzhou, China

In-situ stress is an important indicator for the preferential selection of coalbed methane (CBM) exploration dessert zones, and is a key factor affecting the production capacity of coalbed methane wells. Coal reservoir permeability is one of the key parameters to evaluate the recoverability and modifiability of coalbed methane and reflects the seepage capacity of coal reservoirs. In this study, *in situ* stress data were collected from multiple injection/fall-off tests of multiple parameter wells in western Guizhou province, China. The relationships among parameters such as pore pressure (P_p), closure pressure (P_c), breakdown pressure (P_b), *in situ* stress, coal permeability, and depth were explored. Using Anderson's classification method, the distribution of three different *in situ* stress states was counted. A new simplified model diagram of triaxial principal stress and depth in the study area is proposed by linearly fitting the triaxial principal stress and burial depth. The envelope equation and median equation of the lateral pressure coefficient k -value stress ratio with depth of burial obtained by Brown and Hoek method were calculated using hyperbolic regression algorithm. The k -values were found to be discrete at shallower depths and converge at deeper depths, gradually converging to .65. The control of *in situ* stress on the permeability of coal reservoirs was explored, and a strong positive correlation was found between the permeability and the Z-shaped variation of the lateral pressure coefficient k -values at shallow depths of 1,000 m. Also, the distribution pattern of vertical permeability basically corresponds to the stress transition zone from the strike-slip fault mode to the normal fault mode. The coal seam permeability has a strong sensitivity to effective *in situ* stress (EIS). In this study, the least squares method with multiple fitting of power exponents is applied to analyze the control mechanism of EIS on permeability in depth and reveal a new relationship between permeability and EIS that is different from that considered by previous authors. Summarizing the above research results, the vertical CBM in western Guizhou is divided into three development potential zones, and 400–1,000 m burial depth is the most favorable vertical development zone.

KEYWORDS

coalbed methane, permeability, *in situ* stress, effective stress, optimum development, western Guizhou

Introduction

Coalbed methane (CBM), also known as gas, is a high-quality, clean and easy-to-transport low-cost unconventional energy resource in its own right. Derived from the International Energy Agency (IEA), China has the third largest CBM resource in the world, after the United States and Canada, accounting for 12% of the world's total CBM. Divided by burial depth, the geological resources of CBM less than 1,000, 1,000–1,500 m and 1,500–2,000 m account for 38.8%, 28.8% and 32.4% of the total geological CBM resources in China, respectively (Qin and Gao, 2012; Bi, 2018). Unlike general oil and gas reservoirs, CBM reservoirs are characterized by thin thickness, large reflection coefficient, high fracture density, and exhibit strong anisotropy. Coalbed methane development in China faces two pivotal problems: how to find high-abundance coalbed methane enrichment areas and how to improve coalbed methane extraction efficiency (Qi and Dong, 2017).

Guizhou Province is a major coal and coalbed methane resource storage area in southern China. The latest round of coalbed methane resource evaluation in Guizhou Province shows that the geological resources of coalbed methane in the recoverable coal seams of the Upper Permian containing more than 4 m³/t in Guizhou Province are 3.06×10^{12} m³ (occupying about 10% of the total coalbed methane resources in China), and 92.8% of the resources are distributed in the Liupanshui coalfield, Qianbei coalfield and Zhina coalfield. Western Guizhou is mainly composed of Liupanshui coalfield and Zhina coalfield, the coalbed methane resources of these two coalfields are concentrated in 15 coal-bearing secondary syncline structures, such as Panguan, Gemudi and Tucheng, with typical features of syncline-controlled gas. In terms of regional distribution, it is characterized by “rich in the west and relatively few in the east, north and south”; in terms of vertical distribution, the coalbed methane reserves at a depth of 1,500 m or shallower are 2.56×10^{12} m³, accounting for 83.7% of the province's total (Yi, 1997; Qin and Gao, 2012; Yi et al., 2019; Yang et al., 2020; Gao et al., 2021; Jing et al., 2021).

Stress is defined as the force exerted on a certain area. The force that interacts within the rock medium through contact to deform and produce motion is called *in situ* stress. *In-situ* stress is a natural stress formed in the long arc of geological history without engineering disturbance, formed by various dynamic processes of the Earth, and mainly consists of three parts: overlying rock pressure, tectonic stress and thermal stress. The gravitational stress field is relatively simple and is mainly influenced by the overlying rock mass. Overlying load data are considerable in numerical simulations of fault zones, rock stiffness, and rocks (Karacan et al., 2008; Luke et al., 2010). Thermal stress is the internal stress increment caused by temperature changes within the rock mass, and the effect of such stress is temporarily not considered in this thesis. *In-situ* stress is strongly influenced by gravity and tectonic force, especially related to horizontal tectonic movements. The causes of these tectonic stress fields are very complex. Tectonic stress is extremely irregular and almost impossible to describe with precise resolution because it keeps changing with time (Luke et al., 2010; Qi and Dong, 2017). The factors affecting the state of *in situ* stress in coal reservoirs are tectonic action, burial depth, and coal rock type (Liu et al., 2017).

In-situ stress measurement of coal-bearing strata has been widely applied in underground coal mining, gas accident management, and CBM exploration in many coal-bearing basins in the United States, Australia, China and Canada (Enever and Henning, 1997; Bodden and

Whrlich, 1998; Pashin, 1998; Liu and Harpalani, 2013). Injection/fall-off test (IFOT) method was introduced into China in 1992 and has been developed and employed for a long time. As a momentous parameter for evaluating the stability of underground engineering, *in situ* stress measurement is very important for evaluating the permeability, recoverability and fracturing ability of coal reservoirs (Meng et al., 2010; Wang et al., 2019; Sang et al., 2022). The influence of *in situ* stress is also reflected in areas such as gas content (Bell, 2006; Salmachi et al., 2021), coal structure (Hu et al., 2017; Lv et al., 2021), wellbore track and borehole stability (Zoback et al., 2003; Liu et al., 2004). Stress has three main impacts on CBM exploration and development: stress on coal reservoir pressure and pore and fracture development characteristics; the influence of stress on the series transfer process of desorption, diffusion and seepage of coalbed methane; the influence of stress on the present underground occurrence state and availability of natural fractures, as well as the morphology and extension direction of artificial fractures formed by hydraulic fracturing, etc. (Ni et al., 2010; Liu et al., 2017). Hence, accurate prediction of *in situ* stress features is of great significance to CBM development.

Different scholars have studied the effect of ground stress on reservoir permeability from different aspects, such as the effect of modern ground stress characteristics on permeability (Yuan, 2004; Jasinge et al., 2011); laboratory simulations of the relationship between effective stress and coal reservoir permeability (Vishal et al., 2013; Wu et al., 2017); and numerical simulations of the effect of different stresses on coal reservoir permeability (Tang et al., 2011). *In-situ* stress prediction models have also evolved from simple uniaxial strain models to models that begin to consider the factor of formation stiffness (Enever and Henning, 1997; Pashin, 2007).

Geological background

The Upper Permian is the cardinal coal-bearing stratum in Guizhou, with a coal-bearing area of about 75,000 km² and the best coal-bearing properties, and a variety of deposition types, developing from west to east, in the order of terrestrial, marine-land transition facies and marine deposits (Tang, 2012). The terrestrial and marine zones are located in the area around Weining in northwestern Guizhou and the east area of the Zunyi-Anshun-Xingyi line respectively, with only a few recoverable coal seams, the cumulative recoverable thickness is basically less than 5.0 m, the coal-bearing properties are poor, and the material basis for CBM formation is weak, so it broadly does not possess the value of CBM exploration and development.

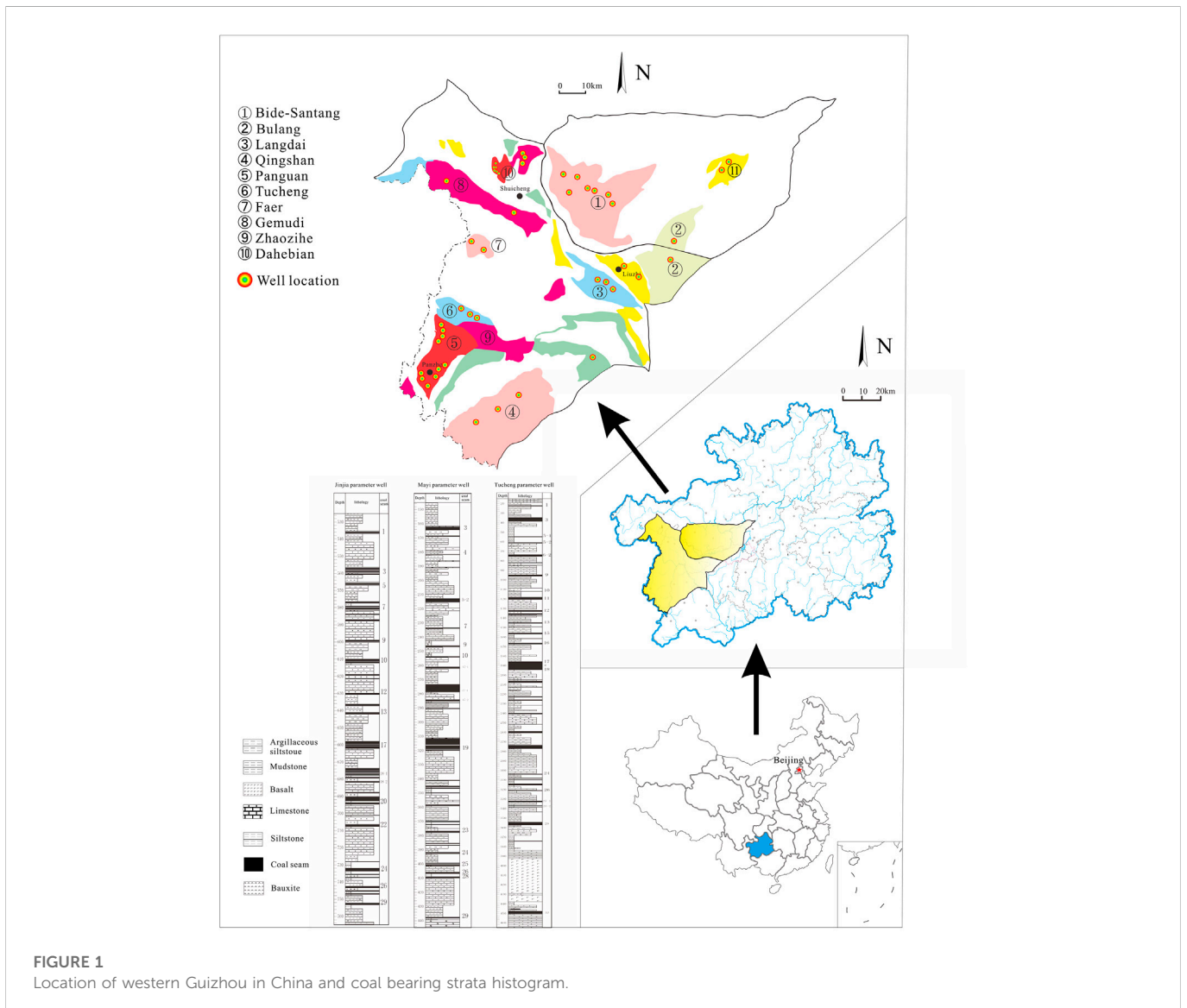
It is a set of sea-land transitional facies coal-bearing deposits consisting of clastic rocks interspersed with carbonate rocks and coal seams, and the main coal-bearing strata are Longtan formation and Changxing formation. The thickness of the Upper Permian coal-bearing system varies greatly (76–543 m), the thickness of single coal seam is thin (generally 1.0–2.5 m), the number of recoverable coal seams and their cumulative thickness vary greatly (0–26 seams, 0–29.8 m), the thin-medium-thick coal seam group is well developed, and contains multiple sections of organic-rich mud shale, and the vertical multilayer phenomenon of gas reservoir is universal. The best material base of CBM reservoirs are mainly located in areas such as Panxian, Shuicheng and Nayong, which generally contain 9–20 recoverable coal seams with a total thickness of 10–30 m,

showing typical characteristics of coal seam group development. By and large, the water-richness of the Upper Permian coal-bearing strata is weak, and there is generally a relative impermeable layer of certain thickness between them and the water-rich limestone aquifer and surface water, and the hydraulic conductivity of fault zones and fracture zones is poor, which is basically difficult to constitute a hydraulic connection channel between coal-bearing strata and strong aquifers or surface water (Gao et al., 2009; Zhao et al., 2019; Gao et al., 2021; Xu et al., 2021).

The gas content of coal seams deeper than 500 m in the Longtan formation in western Guizhou typically ranges from 8.0 to 25.0 m³/t, and the average value is generally about 12.0–15.0 m³/t. For example, in the Bide-Santang basin of the Zhina coalfield, the coalbed methane content in the area varies from .24 to 29.21 m³/t, with a mean of 13.81 m³/t; the coalbed methane content in the Qingshan diagonal area of Liupanshui ranges from 3.87 to 29.16 m³/t, with an average of 12.79 m³/t; the mean coalbed methane content in each area substantially exceeds the 12 m³/t limit of coalbed methane content in the first class area (Yang et al., 2020). In the middle coal-order areas, like Tucheng syncline, the gas content exceeds

12 m³/t, and the gas-bearing saturation generally exceeds 100%, and supersaturated reservoirs occur (Jin et al., 2021; Lu et al., 2022). The distribution of coal-bearing syncline and CBM well location in western Guizhou are shown in Figure 1.

The Late Permian coal-bearing strata in western Guizhou were formed in the Late Permian Longtan stage, and are characterized by “multi-phase development, strong divergence, and late determination” in terms of tectonic evolution, forming a complex tectonic pattern dominated by folds and thrust faults (Dou et al., 2012). The WSM project explored the *in situ* stress field in the study area founded on multiple methods such as seismic source mechanism, hydraulic fracturing and drilling cores. The results display that the δ_{Hmin} in western Guizhou area is mainly the NW-SE direction. There are features such as sea-land interaction, planar divergence and frequent vertical variation in sedimentary development, which are the making of distinctive features of CBM geological conditions. In conclusion, the geological environment of coalbed methane reservoirs in the study area embodies characteristics such as the development of multiple coal seams, thin single layer, large cumulative thickness, multi-layer stacking, relatively concentrated coal seams (small coal



spacing), large structural changes in the coal body, low pore permeability, high stress, and high gas content (Yi et al., 2019; Jin et al., 2021).

Test methods and data processing

Test methods

Coalbed methane well test technology is an important vehicle for understanding coal reservoirs, evaluating reservoir (*in situ* stress measurement), monitoring production dynamic and evaluating completion efficiency. Based on the characteristics of low pressure and low permeability of coal reservoirs. IFOT is widely used as a common well test method in CBM wells. In China, the relevant testing activities are conducted in conformity to the requirements of the national standard GB/T 24504-2009 and GB/T 34229-2017. International standards are not uniform, in the United States is ASTM D5716/D5716M-20, in the United Kingdom is BS ISO 10426-3-2003. In IFOT, the formation pressure is higher than the gas desorption pressure, and the coal seam pore fractures are always saturated with water and in a single-phase flow state.

IFOT, which is utilized in coalbed methane wells in the study area, is a single well pressure transient test. It involves injecting water into the well for a period of time at a more stable discharge, lower than the coalbed rupture pressure, creating a pressure distribution zone around the wellbore, which is above the original reservoir pressure, and then shutting down the well so that the pressure gradually equilibrates with the original reservoir pressure. The test procedure consists of no less than three reopening cycles, each comprising three steps: fluid injection, pump shutdown, and pressure decay. Well testing equipment includes two parts: surface equipment and downhole equipment. The surface equipment mainly includes pumping system, wire winch and wellhead equipment. The main downhole equipment includes electronic pressure gauges, packers and downhole shut-in tools. Well test analysis software mainly includes Saphir 3.20, Pan System V3.4 and so on.

IFOT for CBM wells is categorized into injection/fall-off and *in situ* stress testing. The steps are: lowering the tubing, pressure testing, seating, ball drop pressurization, knocking off the ball seat, lowering the pressure gauge, and water injection testing. After 12.00 h of continuous injection while maintaining a relatively constant

discharge, the well was shut-in to test bottomhole pressure recovery. IFOT pressure and temperature curves are shown in Figure 2A.

Figure 2B signifies the pressure versus flow rate graph in an IFOT. The early stage of the injection phase is the stage of adjusting the discharge volume, the other stages are more stable, and the pressure returns to normal in the recovery phase of the shut-in well with a smooth curve and the most representative analysis of the pressure drop curve. The analysis of test results mainly employs semi-log (Horner) curve and double-log (diagnostic) curve fitting analysis methods, and is supplemented by pressure drop curve fitting to check the analysis results. Namely, the reservoir pressure and pressure gradient of the corresponding coal seam is available. The pressure/time square root curve is the closure pressure at the test point. The rupture pressure is primarily derived from the highest point of the time/pressure curve (Figure 3).

Data processing

In this study, 146 *in situ* stress test data were collected from 49 parameter wells in the present-day CBM hotspot exploration blocks in western Guizhou Province, China. Such data were obtained by IFOT from seven large coal-bearing basins, including the Panguan, Tucheng, Qingshan, and Gemudi synclines. Some of these test data are cited from the literature of Xu et al. (2016). It should be noted that the *in situ* stress data in the literature of Xu et al. are not available from the Panguan and Tucheng synclines, while the main direction of data collection in this study is just the Panguan and Tucheng synclines. Consequently, the data available for the study basically cover the main CBM development areas and exploitation well fields in western Guizhou area, and they are all from the latest exploration and development results since 2014, especially since 2016, which are representative and extensive.

At the minimum compressive stress of the borehole, the conditions for inducing tensile cracks on the borehole are:

$$P_b = 3\delta_h - \delta_H - P_p + T_o \quad (1)$$

Where T_o is the tensile strength of the rock, P_p is the reservoir pressure (pore pressure), and P_b is the rupture pressure. δ_h can be fixed by fracture extension pressure or stopping pump pressure. Bredehoeft

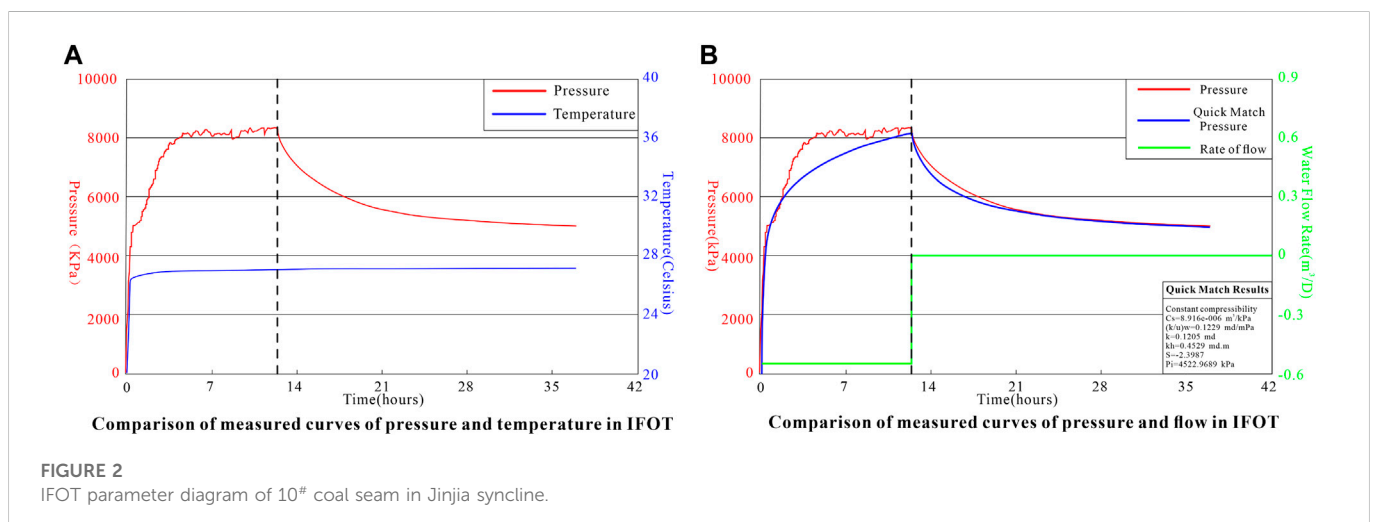


FIGURE 2
IFOT parameter diagram of 10# coal seam in Jinjia syncline.

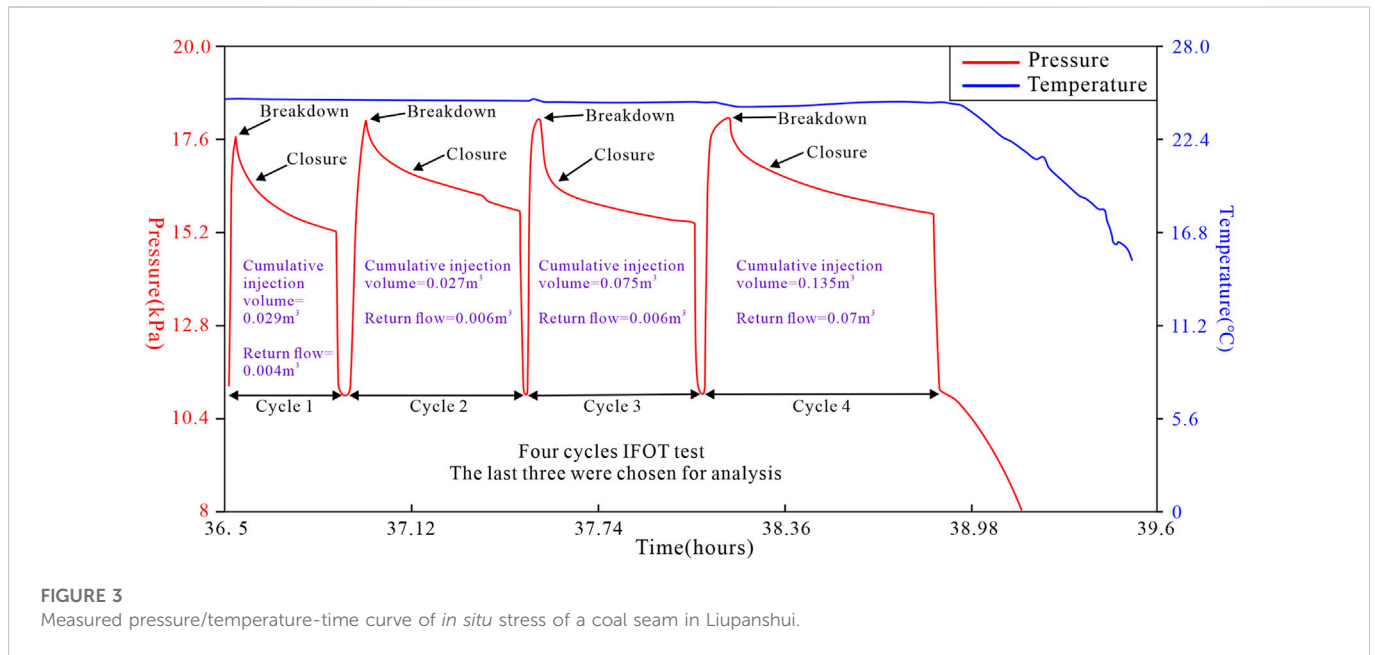


FIGURE 3
Measured pressure/temperature-time curve of *in situ* stress of a coal seam in Liupanshui.

et al. (1976) pointed out that to avoid the determining T_o , two or more pressurization cycles can be adopted and since the coal seam has ruptured in the first reopening cycle, in the subsequent reopening cycle, the tensile strength T_o is zero. The above equation is then simplified as:

$$\delta_H = 3\delta_h - P_b - P_p \quad (2)$$

In IFOT construction, the direction of vertical fracture extension is perpendicular to SH. After the closed hole section is ruptured at the hole wall, the fracture will be extended to depth if the fluid injection and pressurization are continued. If the pump is stopped instantaneously after the formation is fractured, the fracture will stop extending and the fracture gradually tend to close, and the equilibrium pressure in the borehole when the fracture is in the critical closure state is called the closure pressure P_c , which is equal to the sum of the ground pressure P_s when instantaneously stopping the pump and the liquid column pressure P_h in the borehole, i.e., $P_c = P_s + P_h$. Meanwhile, the closure pressure is also equal to the horizontal minimum principal stress δ_h perpendicular to the fracture surface (Haimson and Cornet, 2003). Hence, δ_h (unit: MPa) is calculated as:

$$\delta_h = P_c \quad (3)$$

The δ_v (unit: MPa) is principally derived from the gravity of the overlying seam, and the δ_v of the coal seam can be predicted from the overlying seam (Zoback, 2012). The magnitude of the vertical principal stress can generally be calculated by integration applying density data from the surface to the target depth.

$$\delta_v = \int_0^H \rho(H)g dH \quad (4)$$

ρ is the rock density; H is the depth of burial; g is the acceleration of gravity.

Hoek and Brown (1980) established the relationship between δ_v and depth by collating global *in situ* stress measurements. It has been

widely applied in the prediction of δ_v in different areas. This empirical formula is as follows.

$$\delta_v = 0.027H \quad (5)$$

Where h is the depth of burial in m. This equation can also be used to calculate the rock static pressure in the shallow part of the Earth's crust.

Results

Well test results and analysis

According to 146 IFOT well tests in western Guizhou, the coal seam burial depth is 145.52–1207.33 m (average 649.84 m). The coal seam permeability is in the range of .003–8.1 mD (average .12 mD), which is much lower than that of other CBM development blocks in China and is a typical ultra-low permeability reservoir.

The magnitudes of the absolute values of the three principal stresses (δ_H , δ_h , and δ_v) in the western Guizhou area in the vertical coordinate system can be calculated utilizing Eq. 2; Eq. 3, and Eq. 5, separately. The data from different coal-bearing basins are summarized in Table 1: the maximum horizontal principal stress (δ_H) ranges from 5.38 to 28.83 MPa, with an average of 17.05 MPa, and the maximum horizontal principal stress gradient is 1.21–4.14 MPa/hm, with a mean of 2.23 MPa/hm. Referring to the previous classification criteria for *in situ* stress in Chinese coal fields (Kang et al., 2009), most of western Guizhou (68%) coal seams fall into the medium stress zone, and some of them belong to the high stress zone (Figure 6-1). Compared with other coal-bearing basins on Earth (e.g., Black Warrior basin, Sydney basin, Bowen basin, and Piceance basin), the *in situ* stress in coal reservoirs in Guizhou is greater (McKee et al., 1988; Hillis et al., 1999; Chen et al., 2017; Tavener et al., 2017; Chen et al., 2017). The leading cause of this phenomenon is that Guizhou has experienced multi-period, multi-phase, and multi-directional tectonic movements since the Late Paleozoic coal-forming period, and the tectonic patterns and systems are superimposed over each

TABLE 1 Statistics of well testing and *in situ* stress measurement parameters in main coal bearing basins in western Guizhou, China.

Coal bearing basin	H (m)	P_b (MPa)	G_b (MPa/hm)	P_c (MPa)	G_c (MPa/hm)	P_p (MPa)	G_p (MPa/hm)	δ_H (MPa)	δ_h (MPa)	δ_v (MPa)	P (mD)
Panguan	315–978	8.91–19.99 (13.77)	1.37–2.88 (2.11)	8.00–17.27 (12.25)	1.12–2.63 (1.88)	3.03–10.83 (6.24)	.63–1.31 (.96)	8.63–25.36 (16.72)	8.00–17.27 (12.25)	8.50–26.42 (17.67)	.007–5.05
Qingshan	145.5–876	7.38–20.83 (13.31)	1.53–3.57 (2.39)	6.32–17.53 (11.69)	1.35–2.96 (2.11)	2.45–8.78 (5.73)	.97–1.14 (1.04)	9.13–22.98 (16.21)	6.32–17.53 (11.69)	3.92–23.65 (15.33)	.029–8.1
Yangmeishu	580–806	9–16.68 (12.78)	1.55–2.07 (1.88)	8.35–14.92 (11.37)	1.44–1.85 (1.67)	6.25–7.62 (6.94)	.95–1.20 (1.05)	9.1–20.46 (14.40)	8.35–14.92 (11.37)	15.66–21.76 (18.14)	.03–.07
Dahebian	579.4–1017.1	12.6–26.8 (16.86)	2.04–2.64 (2.23)	12.44–23.21 (15.87)	1.84–2.38 (2.09)	6.67–14.95 (8.92)	1.05–1.50 (1.19)	16.59–28.28 (21.81)	12.44–23.21 (15.87)	15.64–27.46 (20.23)	.034–.173
Tucheng	319.4–1207.3	9.4–25.26 (15.21)	1.8–3.4 (2.31)	7.73–21.2 (13.13)	1.57–2.99 (1.99)	3.19–12.35 (7.37)	.75–1.40 (1.07)	10.12–28.83 (16.81)	7.73–21.2 (13.13)	8.62–32.60 (18.36)	.016–.906
Zhina	291.5–964.1	5.55–21.41 (11.67)	1.61–2.57 (2.11)	4.48–17.52 (9.71)	1.30–2.28 (1.79)	2.34–8.11 (4.47)	.64–.94 (.79)	5.38–23.04 (13.0)	4.48–17.52 (9.71)	7.87–26.03 (14.86)	.003–.053
Avg	145.5–1207.3	5.55–26.8 (14.2)	1.37–3.57 (2.22)	4.48–23.21 (12.63)	1.12–2.99 (1.98)	2.29–14.95 (6.63)	.63–1.50 (1.02)	5.38–28.83 (17.05)	4.48–23.21 (12.63)	3.92–32.60 (17.55)	.003–8.1 (.12)

H (m), burial depth; P_b (MPa), breakdown pressure; G_b (MPa/hm), the gradient of the breakdown pressure; P_c (MPa), closing pressure; G_c (MPa/hm), the gradient of the closing pressure; P_p (MPa), pore pressure; G_p (MPa/hm), the gradient of the pore pressure; δ_H (MPa), maximum horizontal principal stress; δ_h (MPa), minimum horizontal principal stress; δ_v (MPa), vertical stress; P (mD), reservoir permeability.

other, and the shallow tectonic deformation in western Guizhou is typical thin-skinned tectonics, so the residual tectonic stresses are stronger. The secondary reason is that the present-day crustal motion in western Guizhou is chiefly influenced by the regional geotectonic context of the eastward extrusion of the Yangzi plate from the Tibetan plateau, and the maximum principal stress direction is more discrete, mostly in the near EW and NEE directions (Zhu, 2018), and the majority of the coal-bearing basins are still in a relatively active stage of crustal evolution with high *in situ* stress and large geothermal gradients (Gao et al., 2021).

Discussion

Analysis of in-situ stress state

Of the 146 data, 89 data that were confirmed at the data collection sites were selected to analyze the pattern of *in situ* stress changes in the vertical direction in accordance with six different coal-bearing synclines. Anderson (1951) analyzed the contributing factors of faults in the perspective of the stress states of fault formation, and proposed three stress states for the formation of normal faults, reverse faults, and strike-slip faults. In this study, adopting Anderson's classification method, the distribution of the three divergent *in situ* stress states in the western Guizhou area was counted (Table 2; Figure 4), and the results are as follows:

1) δ_H dominates 48.3% of the measurement points, and δ_v dominates 51.7% of the measurement points. The two are almost equal. Further statistics reveal that the inverse fault stress pattern represented by $\delta_H > \delta_h > \delta_v$ has only four data, accounting for 4.49%. The strike-slip fault represented by $\delta_H > \delta_v > \delta_h$ has 39 data, making up 43.82% of the total

data. The normal faults represented by $\delta_v > \delta_H > \delta_h$ have 46 data, occupying 51.69% of the total data. Consequently, the stress environment in the study area generally shows a state of strike-slip fault and normal fault, and basically does not show a state of reverse fault. The regional geological background survey also shows that the study area does not develop retrograde thrust structures.

2) In the Panguan syncline, the shallow *in situ* stress mainly exhibits the state of strike-slip fault (<650 m), and the deep *in situ* stress mainly displays the state of normal fault (>550 m). It is noteworthy that the depth range of 550–650 m is the zone of complex stress changes, and both strike-slip fault state and normal fault state occur. In the depth range of 527–558 m and 569–611 m, the magnitudes of δ_H and δ_v are basically equal, and the *in situ* stress state is close to $\delta_H \approx \delta_v > \delta_h$, which is the stress transition zone from $\delta_H > \delta_v > \delta_h$ to $\delta_v > \delta_H > \delta_h$. In the Qingshan syncline, the depth range of 500–600 m is the stress complex change zone, and both strike-slip fault state and normal fault state occur. The stress transition zone is located at 689–721 m, which is more characteristic of strike-slip fault at this depth, and there are only a few data on the Yangmeishu syncline, and the *in situ* stresses and *in situ* stress gradients are low, showing the features of regional and vertical low anomalies of *in situ* stresses. The vertical principal stresses always dominate the direction and development pattern of the *in situ* stress, and all the measured points present normal fault state; the Dahebian syncline has no reverse fault state distribution (sporadic development of strata in the very shallow part cannot be excluded), and a tremendous amount of strike-slip faults are distributed from shallow to deep, and the stress transition zone is located at 592–695 m. In the deeper part of the syncline

TABLE 2 *In situ* stress distribution in different coal bearing basins in western Guizhou.

Basins	Data volume	Depth	Anderson type	Proportion (%)	Corresponding depth
Panguan	32	315–978 m	$\delta_H > \delta_h > \delta_v$	3.10	<350 m
			$\delta_H > \delta_v > \delta_h$	46.90	450–650 m
			$\delta_v > \delta_H > \delta_h$	50.00	>550 m
Qingshan	15	145.5–876 m	$\delta_H > \delta_h > \delta_v$	6.70	<250 m
			$\delta_H > \delta_v > \delta_h$	46.70	250–600 m
			$\delta_v > \delta_H > \delta_h$	46.70	>500 m
Yangmeishu	6	580–806 m	$\delta_H > \delta_h > \delta_v$	0	None
			$\delta_H > \delta_v > \delta_h$	0	None
			$\delta_v > \delta_H > \delta_h$	100.00	550–800 m
Dahebian	14	579.4–1017.1 m	$\delta_H > \delta_h > \delta_v$.00	None
			$\delta_H > \delta_v > \delta_h$	78.60	550–1000 m
			$\delta_v > \delta_H > \delta_h$	21.40	700–900 m
Tucheng	14	319.4–1207.3 m	$\delta_H > \delta_h > \delta_v$	7.10	<350 m
			$\delta_H > \delta_v > \delta_h$	21.40	350–400 m
			$\delta_v > \delta_H > \delta_h$	71.40	>400 m
Zhina	8	291.5–964.1 m	$\delta_H > \delta_h > \delta_v$	12.50	<300 m
			$\delta_H > \delta_v > \delta_h$	37.50	300–600 m
			$\delta_v > \delta_H > \delta_h$	50.00	>450 m

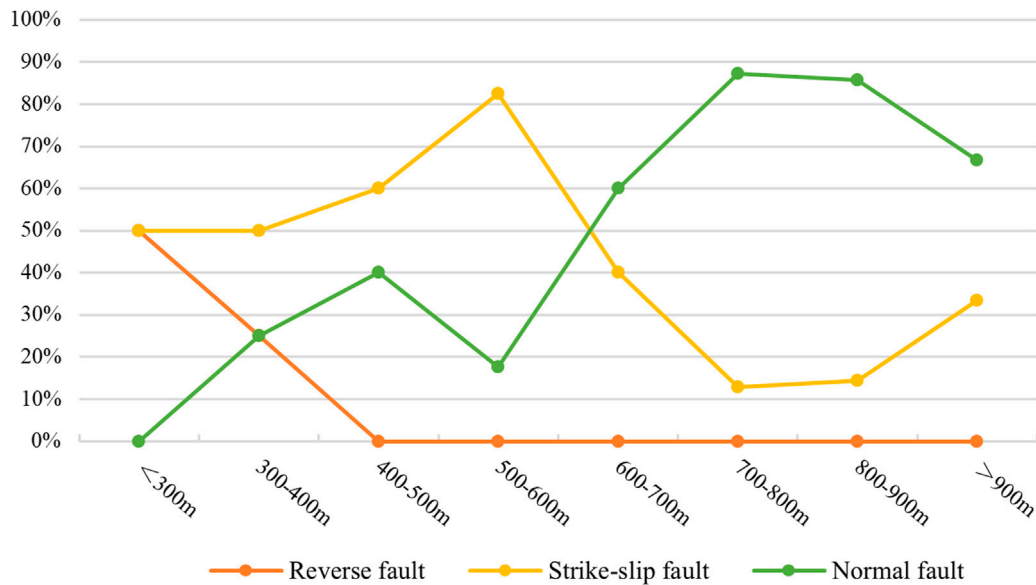


FIGURE 4
Proportion of different *in situ* stress states at different depths.

(>900 m), the stress state tends to be strike-slip-normal fault property. In the Tucheng syncline, the normal fault state is the dominant stress state, accounting for 71.40% of all measured data. 384–441 m is the stress transition zone, and the area deeper than 900 m tends to have the strike-slip-normal fault property. The zone of complex stress change in the Zhina coalfield is located in the deep range of 450–600 m. Although the percentage of reverse fault data is the highest among all coal-bearing basins (12.50%), this is caused by the small amount of total data in Zhina coalfield, and its *in situ* stress development pattern is basically consistent with the nearby coalfields.

- 3) The reverse fault stress state normally appears only in the shallow part (<400 m), and disappears rapidly with the increase of depth. The strike-slip fault stress state is distributed at varied depths, with a higher percentage at 400–600 m depth. The normal fault stress state occurs less in the shallow strata and increases rapidly beyond 600 m to become the main stress state, where the vertical stress is the greatest and the strata are the most stable. For strata over 400 m, strike-slip faults are strictly negatively correlated with normal faults. In deep strata, the stress state is prone to have the property of strike-slip fault because $\delta_H \approx \delta_v > \delta_h$. Kang suggests that the increased occurrence of strike-slip fault types in deep strata is the result of strong geotectonic movement in the horizontal direction (Kang et al., 2010).

Variation relationship between in-situ stress and burial depth

The pressure cycling tests of CBM parameter wells in the western Guizhou area also obtained data related to rock breakdown pressure (P_b), closure pressure (P_c) and pore pressure (P_p). These pressure data are also the key parameters for subsequent CBM development. The pore pressure P_p is 2.29–14.95 MPa (average 6.63 MPa), and the pore

pressure gradient (G_p) is .63–1.50 MPa/hm (average 1.02 MPa/hm), so it is a normal pore pressure reservoir. The rock breakdown pressure P_b is 5.55–26.8 MPa (average 14.2 MPa), and the breakdown pressure gradient (G_b) ranges from 1.37–3.57 MPa/hm (average 2.22 MPa/hm). The deep pore pressure values are usually related to hydrostatic pressure, which increases at a fixed rate of 10 MPa/km with the increment of depth. The upper limit of pore pressure is the overlying formation pressure δ_v , and the pore pressure is always less than the minimum principal stress δ_3 (the smallest principal stress in the triaxial principal stress).

The pore pressure, closure pressure and breakdown pressure of different coal-bearing synclines at varied depths in western Guizhou area exhibit a linear increasing trend with the deepening of depth (Figure 5). The correlation coefficients are all above .67 with good correlation. Such relationship is similar to that of the Qinshui basin in China (Meng et al., 2010). In particular, the correlation between breakdown pressure and closure pressure is very good, with correlation coefficients being above .9. The tight positive correlation between closure pressure and breakdown pressure reflects the crucial influence of the tectonic stress field on the pressure of coal reservoirs, i.e., a very large share of the fluid energy in coal seams from the transfer of *in situ* stress, not all of which is contributed by the underground water dynamic field.

In further discussion, this study found that the calculated results of the *in situ* stress test wells contain more important fundamental relationships between reservoir physical parameters. This study focused on the relationship between triaxial principal stress and depth. δ_H is linearly and positively correlated with burial depth (Figure 6A), and δ_h is linearly and positively correlated with burial depth (Figure 6B). However, the correlation coefficients R^2 are relatively small, indicating that the horizontal principal stresses in multiple directions are not highly correlated with depth. Figures 6C, D demonstrate the relationship between depth and horizontal principal stress gradient. It can be found that in any depth range below the surface, both points with higher and lower gradients are distributed

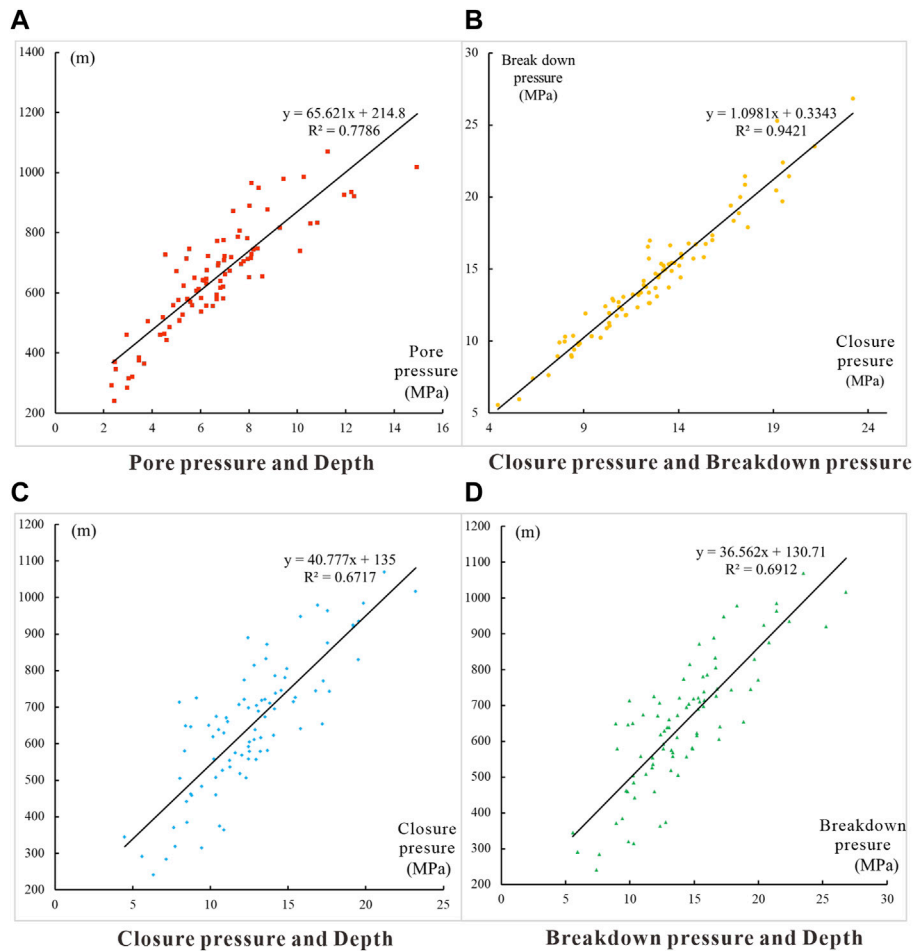


FIGURE 5

The relationship between pore pressure and depth (A), closure pressure and breakdown pressure (B), closure pressure and depth (C), breakdown pressure and depth (D).

concurrently with a wide range span. This sidewise proves that the relationship between horizontal principal stress and depth H is more discrete. Hence, the relevant data of δ_H , δ_h and δ_v in western Guizhou area are projected uniformly into Figure 7.

The yellow straight line in Figure 7A represents the hydrostatic pressure, and the minimum principal stresses in coal reservoirs at varied depths in different zones of the study area are greater than the corresponding hydrostatic pressures at that depth to avoid possible hydraulic fracturing of the reservoir, which is consistent with the situation summarized by Zoback (2012) after studying the Rocky Mountains, Gulf of Mexico oil fields, and North Sea oil fields in the United States. The gray line denotes the vertical principal stress δ_v . The orange line means the linearly fitted trend line for the minimum principal stress δ_h . The dark blue line stands for the linearly fitted trend line of the maximum principal stress δ_H . It can be noticed that founded on the definition, the gray straight line will pass through the origin of the cross coordinate system and both the orange and blue straight lines intersect the negative half-axis of the Y-axis. Figure 6E shows that δ_H has a very high correlation with δ_h , which can be corroborated from Figure 7A. The slope difference between the orange and blue straight lines is small, indicating the high consistency of the minimum principal stress and maximum principal stress with the

variation of depth. In the premise of the above perception, this study redrew the simplified mode diagram of relationship between triaxial principal stress and depth in western Guizhou region, which is shown in Figure 7B. In western Guizhou region, δ_H and δ_h are highly correlated and change synchronously, and the gradient of δ_v change is more than the two horizontal principal stresses. As a result, in the shallow stratum within H_1 , the *in situ* stress mostly shows the inverse fault pattern. In the deeper strata over H_2 , the *in situ* stress mostly shows the normal fault mode. In the area between H_1 and H_2 , the triaxial stress values are close to each other and the stress types are complex, which is regarded as an important transition zone of the *in situ* stress. This is simultaneously in full agreement with the statistical pattern of *in situ* stress described previously (Table 2; Figure 4).

The distribution of stress ratio with depth and the establishment of hyperbolic regression relationship

In mathematical statistics, regression analysis focuses on the search for approximate functional relationships between variables (Chen, 2009). Assuming that there is a dependent variable y and

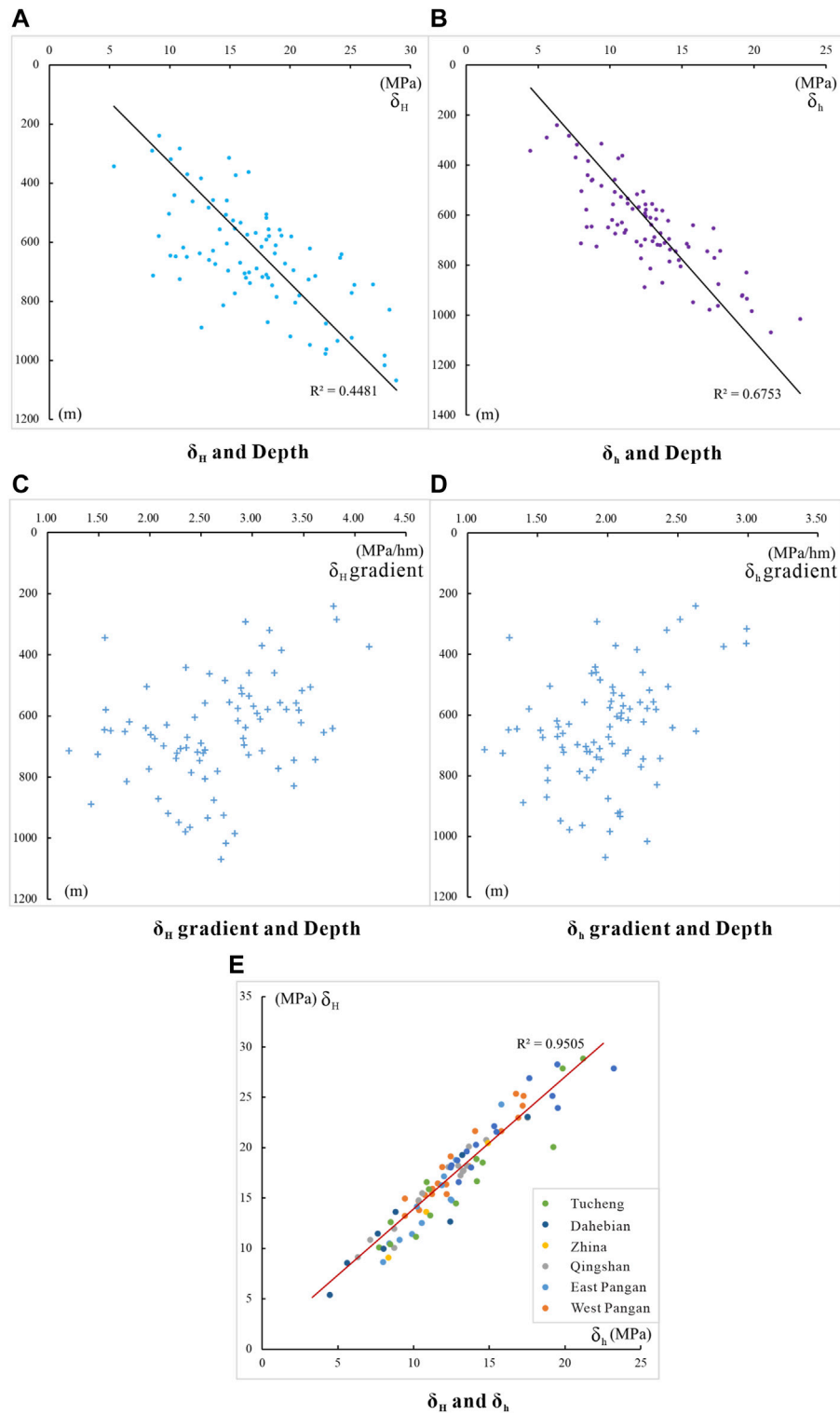


FIGURE 6
Relationship between δ_H and depth (A), δ_h and depth (B), δ_H gradient and depth (C), δ_h gradient and depth (D), δ_H and δ_h (E).

an independent variable x_1, x_2, \dots, x_n in a problem, it is conceivable that the value of y consists of two components.

One part, due to the influence of x_1, x_2, \dots, x_n , which is denoted as a function of x_1, x_2, \dots, x_n in the form $f(x_1, x_2, \dots, x_n)$. The other part, which is due to the influence of numerous other unconsidered

factors, including random factors, can be regarded as a random error, noted as b .

Obtain the model:

$$y = f(x_1, x_2, \dots, x_n) + b \tag{6}$$

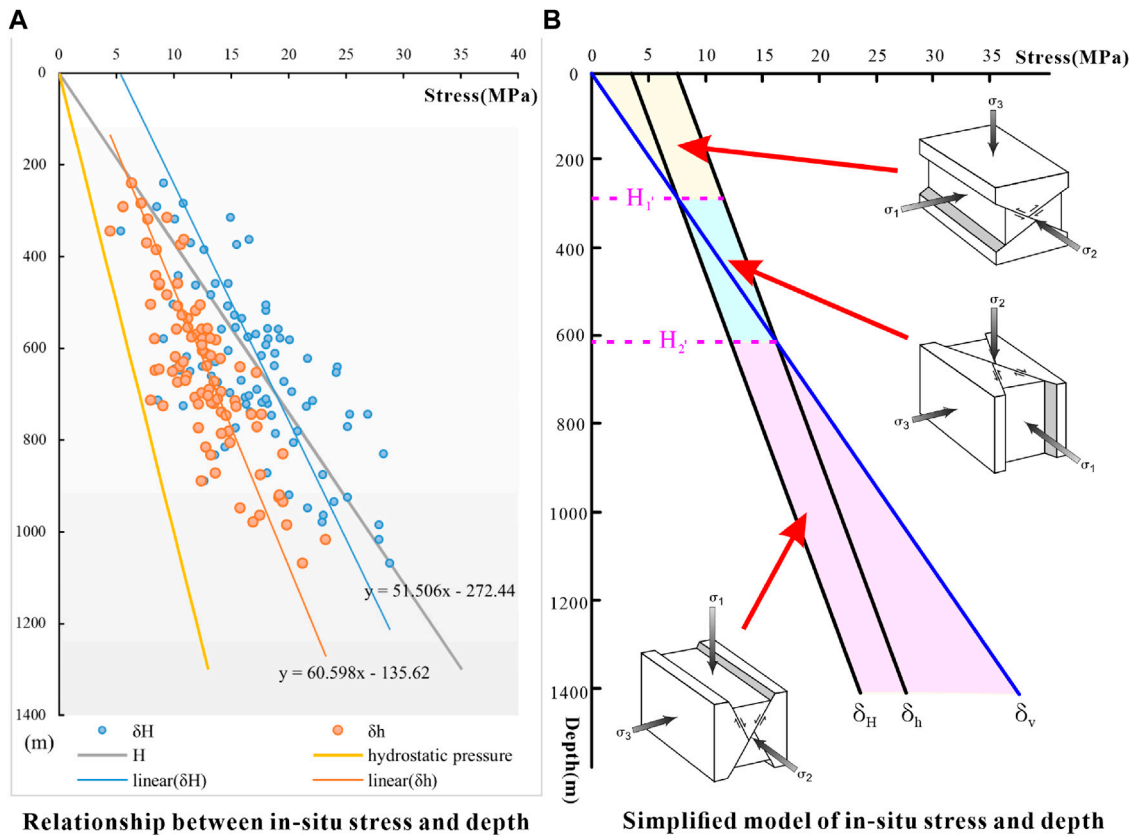


FIGURE 7
Relationship between triaxial *in situ* stress and depth in western Guizhou.

The function $f(x_1, x_2, \dots, x_n)$ is called the “regression function” of y on x_1, x_2, \dots, x_n . The regression function is a hyperbolic case, called hyperbolic regression.

In studying the variation of the *in situ* stress field, the lateral pressure coefficient k is often used to describe the state of *in situ* stress at a point (Brown and Hoek, 1978). The k is an effective parameter to characterize the distribution of *in situ* stress. It varies in different parts of the world, and its value usually ranges from .5 to 5, with most of the distribution between .8 and 1.5 (Han et al., 2012). The k is defined as follows (Brown and Hoek, 1978; Chen et al., 2017; Chen et al., 2018):

$$k = \frac{(\delta_H + \delta_h)}{2\delta_v} \tag{7}$$

From the definition, k value is the ratio of the average horizontal principal stress to the vertical stress, which is an effective parameter to characterize the distribution of *in situ* stress (dimensionless). Similarly, there are K_H and K_h which indicate the relationship between the mutual magnitude of *in situ* stress. The former indicates the ratio of the maximum horizontal principal stress δ_H to the vertical principal stress δ_v , and the latter indicates the ratio of the minimum horizontal principal stress δ_h to the vertical principal stress δ_v .

According to the previous study in this paper, δ_H , δ_h and δ_v are all linearly related to depth. The relationship between δ_H , δ_h and δ_v and depth H can be described as:

$$\delta_H = a_1 \times H + b_1 \tag{8}$$

$$\delta_h = a_2 \times H + b_2 \tag{9}$$

$$\delta_v = 0.027 \times H \tag{10}$$

a_1, b_1, a_2, b_2 are the coefficients to be determined for the primary function and H represents the depth.

Combining Eqs 7–10, it is obtained that:

$$k = \frac{b_1 + b_2}{0.054H} + \frac{a_1 + a_2}{0.054} \tag{11}$$

Let $m = \frac{b_1 + b_2}{0.054}$, $n = \frac{a_1 + a_2}{0.054}$

Eq. 11 is equivalent to:

$$k = \frac{m}{H} + n \tag{12}$$

It can be found that Eq. 12 is a hyperbola with eccentricity of 2, which is exactly the relationship used by Hoek-Brown in the regression analysis of the lateral pressure coefficient. According to Eq. 12, the value of lateral pressure coefficient k is linearly related to the inverse of the depth.

Brown and Hoek (1978) summarized the results of *in situ* stress measurements around the world and found that the ratio of the average horizontal stress to the vertical stress, k , usually falls within the following defined range:

$$\frac{100}{H} + 0.3 \leq k \leq \frac{1500}{H} + 0.5 \quad (13)$$

The average value of k in this equation is:

$$k = \frac{800}{H} + 0.4 \quad (14)$$

Similarly, some Chinese scholars have summarized the range of variation of lateral pressure coefficient of *in situ* stress in China and the variation law with depth according to Hoek-Brown's method (Zhao et al., 2007; Jing et al., 2008). The lateral pressure coefficient of Chinese sedimentary rocks is usually in the following range:

$$\frac{54}{H} + 0.2 \leq k \leq \frac{1500}{H} + 0.5 \quad (15)$$

The average value of the *in situ* stress k in sedimentary rocks in China is:

$$k = \frac{124}{H} + 1 \quad (16)$$

The coefficients in Eqs 8, 9 can be obtained by linear regression analysis of *in situ* stress measurements in western Guizhou (Figure 8), $a_1 = .0187$; $b_1 = 4.92$; $a_2 = .0164$; $b_2 = 1.93$. Eq. 12 becomes:

$$k = \frac{126.9}{H} + 0.65 \quad (17)$$

The overall data for the hyperbolic regression analysis of the *in situ* stress in western Guizhou come from 92 sets of valid *in situ* stress data from multiple parameter wells in several coal-bearing basins in the western Guizhou region, leaving 87 sets of data after removing error data that deviate significantly from the normal range. The k -values of the overall western Guizhou *in situ* stress data range from .39 to 1.95, with a mean value of .94. Eq. 17 shows the median curve of the k -values of the western Guizhou *in situ* stress, and in Figure 9A, the red dashed line represents the median curve of the western Guizhou *in situ* stress. According to the method of Hoek-Brown and other scholars (Brown and Hoek, 1978; Zhu and Tao, 1994; Jing et al., 2007; Wang et al., 2012), the range of western Guizhou *in situ* stress lateral pressure coefficient according to the available data is as follows:

$$\frac{40}{H} + 0.4 \leq k \leq \frac{300}{H} + 0.73 \quad (18)$$

The lateral pressure coefficient k value reflects the strength of the horizontal stress relative to the vertical stress. The relationship between k value and depth in western Guizhou area is shown in Figure 9A. The k value exhibits a wide and complex variation in shallow strata, and its range of values gradually shrinks with the augmentation of depth. Meanwhile, the contraction rate of k value also decreases with depth. In general, it shows the feature of "dispersion at the shallow part and convergence at the deep part." In Figure 9B, the red curve is the characteristic curve of the left part of Eq. 13, which is called Hoek-Brown outer envelope; the green curve is the characteristic curve of the right part of Eq. 13, which is called Hoek-Brown inner envelope, and it is also the characteristic curve of the right part of Eq. 15, which is called Chinese sedimentary rock inner envelope; the black curve is the characteristic curve of the left part of Eq. 15, which is called Chinese sedimentary rock outer envelope; the blue dashed line corresponds to Eq. 16, which is the median curve of Chinese

sedimentary rocks. Apparently, the k value envelopes of Chinese sedimentary rocks all lie within the Hoek-Brown envelope, and the trends of the two sets of curves are relatively similar. The relationship between k values and H obtained from the western Guizhou stratum is also similar to that of the southern Qinshui basin (Meng et al., 2011) and the eastern Liulin area of the Ordos basin (Li et al., 2014) in China, although there are huge differences in the quantitative values. This sideway proves again that the vertical variation of k is hyperbolic in shape. The measured values of *in situ* stress in the western Guizhou area all lie within the Hoek-Brown envelope, but are clearly biased toward the smaller end, with 97.7% of the data being smaller than the median curve for Chinese sedimentary rocks, except for two groups of *in situ* stresses.

Statistically, in the coal-bearing basins of western Guizhou region, $k < .86$ is the basic normal fault type for the nature of *in situ* stress; $.86 < k < 1.2$ is the basic strike-slip fault type; and $k > 1.2$ is the basic reverse fault nature. In the depth range within which data are available, the minimum value of k occurs in the range of 600–900 m, which is about .4–.6, but also within this depth range, the k values of many recorded points are still large. This indicates that in some coal-bearing strata in this range, the overlying stress is much greater than the tectonic stress, and the tectonic residual stress is weak (Engelder, 1993). Empirically, the overlying stresses do not change abruptly with depth, which should be the result of the sudden drop of local tectonic pressure due to the unique multi-seam stacking and multi-level closed pore pressure system in the western Guizhou area. The sudden drop in tectonic pressure brings about a rapid decrease in reservoir permeability and complex changes in the direction and magnitude of the main *in situ* stress, adding massive uncertain control factors to the reservoir transformation and fracturing construction design. Within the depth range of 800–1,100 m, the k value has a tendency to increase gradually, and the average horizontal stress at this time, although still smaller than the vertical stress, is slowly approaching the value, and the normal fault nature of the *in situ* stress is gradually transitioning to the nature of the strike-slip fault. At this point, the stratigraphic position collected by IFOT is relatively close to the core of the coal-bearing stratigraphic syncline. The geotectonic framework of the western Guizhou area indicates that the area is characterized by the alternative distribution of syncline-anticline and the tight closure of syncline. The strata located near the core of the syncline are in a stress environment where the lateral extrusion stress increases rapidly, resulting in an abnormal increase of k value. After calculation, the k value is generally less than 1 for strata with burial depths greater than 800 m. The data with $k > 1.2$ exist only in strata with burial depths less than 400 m. The average value of k is .1. And the average value of k value is .94, which is similar to the results calculated by Chen (Chen et al., 2017). Hence, the *in situ* stress type in western Guizhou area is dominated by the coexistence of the strike-slip fault type and the normal fault type in the transition zone, and the normal fault type in the deep part, with the least percentage of the reverse fault type.

The presence of the inner and outer envelopes makes it possible to infer the variation of the depth *in situ* stress parameters. Combining Eq. 7, Eq. 16 and Eq. 18, the value of k gradually decreases with the increase of depth and tends to stabilize and converge. The ratio of the average horizontal principal stress to the vertical stress decreases toward a fixed value, $k \rightarrow .65$. The range of k values at a certain depth underground can also be obtained by Eqs 17, 18. For instance,

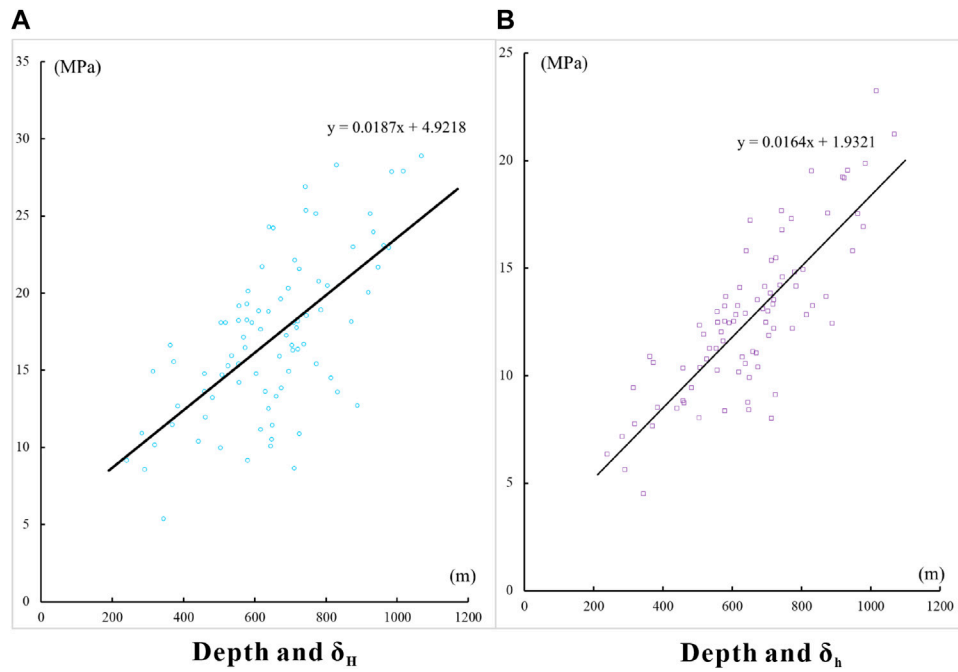


FIGURE 8
The relationship between depth and δ_H (A), depth and δ_h (B).

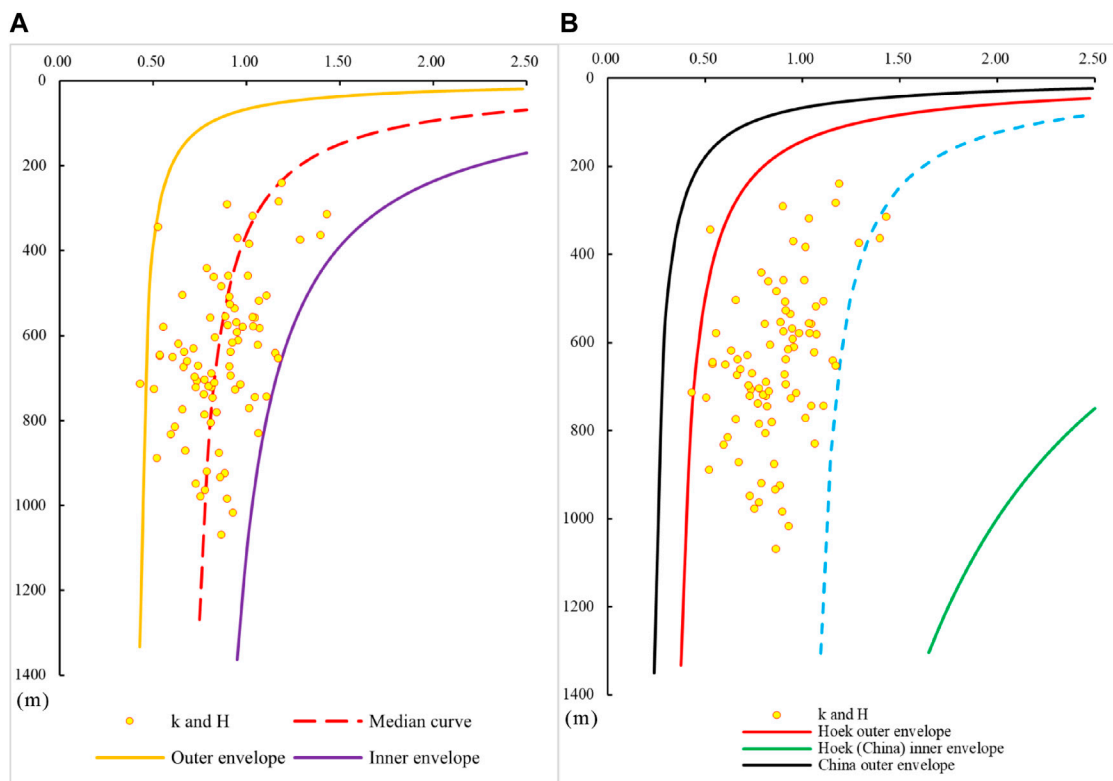


FIGURE 9
Hyperbolic fitting relationship between k value and depth in western Guizhou.

the inferred value of k at 2 km depth is between .42 and .88, with an average value of .71. The vertical stress is about 54 MPa on the basis of the gravity of the overlying rock layer, so the average horizontal principal stress at 2 km depth can be inferred to be between 22.68 and 47.52 MPa, with a mean value of 38.34 MPa. This provides a theoretical reference for the upcoming ultra-deep coal seam gasification and reservoir reformation operations.

Influence of in-situ stress field on coal permeability

Coal reservoir permeability is one of the cardinal parameters for evaluating the recoverability and fracturing ability of coalbed methane, reflecting the seepage capacity of coal reservoirs (Sun et al., 2017). Permeability measures the difficulty of fluid passing through the reservoir. Coal seam is a typical dual pore medium consisting of a matrix pore-fracture system, so coal seam permeability includes matrix pore permeability and fracture permeability; the latter is the main source of coal reservoir permeability (Pan and Luke, 2017; Men et al., 2021). The distribution pattern of natural fractures is controlled by the paleotectonic stress field, while the modern *in situ* stress field chiefly controls the degree of natural fracture opening, which further affects permeability (Liu et al., 2017). In addition to the factors affecting reservoir permeability, such as geological structure, *in situ* stress, burial depth, and coal structure, the effective stress effect, coal matrix shrinkage effect, and gas slip effect also act together on coal reservoir permeability during drainage and depressurization (Fu et al., 2007; Wang et al., 2012). Currently, the influence on reservoir permeability is mainly studied from aspects such as reservoir stress sensitivity (Chen et al., 2011; Xue et al., 2015), fracture compression coefficient (Xue et al., 2015), coal sample deformation (Zhou et al., 2009; Guo, 2012), pore pressure (Zhou et al., 2009) and different coal ranks (Xue et al., 2015). Among the many influencing factors, the effect of effective stress on permeability is conspicuous and always present. Profuse studies have shown that the coal permeability is not only related to the stress in one direction, but also depends on the influence of the main stress in three directions (Luke et al., 2010; Meng et al., 2011; Pan and Luke, 2017).

On account of the special geological situation of western Guizhou region, the lateral pressure coefficient of Eq. 6 is selected as a representative of the *in situ* stress in three directions, and its relationship with the variation of permeability in the vertical direction is analyzed (Figure 10). The value of lateral pressure coefficient k reflects the strength of horizontal stress relative to vertical stress. $k > 1$, the horizontal stress is dominant at this time; $k < 1$, the vertical stress is dominant. Compared with other large CBM development regions in China, the reservoir permeability in the study area is generally low, with test well permeability being $(.001-.5) \times 10^{-3} \mu\text{m}^2$ (Gao et al., 2018). Even plenty of points with permeability less than $(.01-.5) \times 10^{-3} \mu\text{m}^2$ (accounting for 18.6%) appear. With the increase of burial depth, the variation of permeability exhibits a trend of increasing first and then decreasing (blue curve in Figure 10). The depth of the reservoir with higher permeability is roughly located at 300–650 m, which basically coincides with the depth where the reverse fault stress mode and the strike-slip fault stress mode exist in large numbers as described in the previous section. The rapidly declining zone of permeability at 600–700 m also basically corresponds to the stress transition zone from the strike-slip fault mode to the normal fault mode. Lateral pressure coefficient k varies

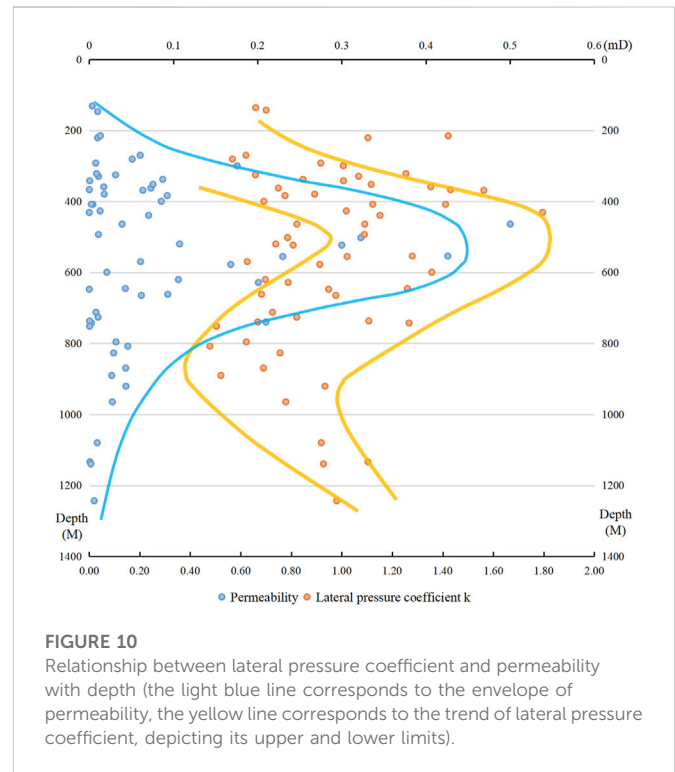


FIGURE 10
Relationship between lateral pressure coefficient and permeability with depth (the light blue line corresponds to the envelope of permeability, the yellow line corresponds to the trend of lateral pressure coefficient, depicting its upper and lower limits).

more complicatedly from shallow to deep, roughly showing a Z-shaped trend of increasing first, then decreasing, then increasing again (yellow curve in Figure 10). At a depth of 1,000 m or less, the high value of lateral pressure coefficient corresponds to the high value of permeability, and the low value of lateral pressure coefficient corresponds to the low value of permeability, and there is a strong positive correlation between the magnitude change of lateral pressure coefficient and permeability. In other words, the magnitude of the average horizontal stress is comparatively synchronized with the change of permeability, and the coal seam with high horizontal stress corresponds to higher permeability, while the coal seam with high vertical stress corresponds to lower permeability.

Griffith (1920) found early that in brittle rocks, when the direction of local stress coincides with the main expansion direction of rock fractures or at a small angle, the fractures will be in tension and the fractures will also continue to expand along the direction of *in situ* stress or brittle rupture will occur in rocks that have not ruptured yet (Griffith criterion of brittle). Qin et al. (1999) developed the application of such criterion in coalfield geology, where the greater the difference in principal stress, the greater the tension effect and the continued expansion of rock fracture volume, which favors the increase in permeability. However, when the local stress direction is perpendicular to the expansion direction of the dominant fractures in the rock, the fractures are compressed and the permeability decreases. Yang et al. (2020) studied coal fields in North China and concluded that the minimum horizontal principal stress δ_h has the greatest impact on permeability, which is also stemmed from the idea that in the direction of δ_2 , the formation will undergo marked Coulomb shear rupture.

Liu et al. opined that the permeability parallel to rock strata is much higher than the permeability perpendicular to rock strata, and the ratio of their absolute values is roughly 4:1 (Chen et al., 2017; Liu et al., 2019). A further study of the physical properties of coal seam reservoirs in the Liupanshui area of western Guizhou by Cheng et al.

concluded that the face cuttings of coal seams are predominantly distributed vertically, with shorter extensions of cuttings, less penetration of layers and gangue, and insufficient vertical connectivity. Nevertheless, in the bedding direction, the strip structure is developed, and the pore fissures between layers and coal rock components are large and long, with good connectivity, so the permeability parallel to rock strata of the coal seam is better (Cheng et al., 2015). Hence, in Figure 10, the points with larger lateral pressure coefficient correspond to the stratum with high horizontal stress, and are also in conformity with the Griffith rupture environment where the continuous expansion of the parallel to rock strata fractures occurs, resulting in the improved permeability parallel to rock strata of the reservoir and the overall permeability of the reservoir. On the contrary, in terms of the points with smaller lateral pressure coefficient at 650–1,000 m, due to the dominant effect of vertical stress, which greatly compresses the volume of parallel to rock strata fracture, and the pore-fracture structure, cut-off system, gas-water transport and percolation field of coal rock are destroyed together, and the permeability of coal reservoir decreases extremely rapidly. It is noteworthy that there are still a multitude of points in Figure 10 that do not match or even are completely opposite to the above summarized patterns, especially the extensive development of ultra-low permeability reservoirs in the western Guizhou coal seam, and the reason for the extremely low permeability of these coal seams seems to have little relationship with the lateral pressure coefficient. Luke, Fu and other researchers, through coal rock physical simulation experiments, pointed out that in underground coal seams, coal rock permeability variation is controlled by the integrated negative effect of effective stress and positive effect of coal matrix shrinkage; the coupling of the two complicates the variation of permeability (Fu et al., 2002; Luke et al., 2010; Pan and Luke, 2017). In Figure 10, the permeability is extremely low in the deep coal seams greater than 1,000 m. The increase of burial depth makes the vertical *in situ* stress become the dominant stress, which leads to the increase of fluid pressure (pore pressure), the effective stress will decrease sharply, and the elastic expansion of coal body makes the fracture narrow and the permeability decrease. Moreover, because of the deeper burial depth and higher local geothermal gradient, the reservoir physical properties shift to the direction of tectonic coal, the coal body structure is fragmented, the original cuttings system, and the seepage channels are completely destroyed, and the permeability decreases exponentially (Qin and Gao, 2012; Hu et al., 2017). The relationship between permeability and lateral pressure coefficient tends to disappear.

The concept of effective *in situ* stress (EIS) was first propounded by Terzaghi (1923), who pointed out in his work on geotechnics that the behavior of saturated rocks is controlled by the EIS (difference between external stress and internal pore pressure). In other words, the *in situ* stress in a coal reservoir is partly borne by the fluid in the pores and fractures of the reservoir, which is called pore pressure or reservoir pressure, and partly borne by the coal matrix, which is called EIS. Nur and Byerlee (1971) developed this concept by proposing an “exact” EIS law, incorporating Biot’s (Biot, 1962) constant into the equation, which can well explain volumetric strain.

$$\delta_{ij} = S_{ij} - \theta_{ij} \alpha P_p \quad (19)$$

Areas where apparent tectonic extrusion is present, pore pressure prediction requires knowledge of all principal stresses. In these areas, applying the average EIS increment ($\delta_H + \delta_h + \delta_v/3 - P_p$) can predict the

porosity reduction more accurately (Qin and Gao, 2012; Zoback, 2012). A great many research scholars in China have concluded through their studies that coal seam permeability in coal-bearing basins such as Qinshui basin, Ordos basin, etc. is extremely sensitive to EIS, and coal seam permeability decreases with the augmentation of EIS, with a good negative exponential power function relationship between the two (Yin, 2014; Chen et al., 2017; Liu et al., 2019). A lot of scholars have established theoretical models of EIS and permeability, and the Palmer-Mansoori (P-M) model (Palmer and Mansoori, 1998) and the Shi-Durucan (S-D) model (Shi and Durucan, 2005) are two common models utilized to simulate reservoir gas transport. The above models apply the two assumptions of a uniaxial stress state and a constant overburden pressure or circumferential pressure to simplify their derivation and derive a simple equation that facilitates the expression of permeability. The permeability of coal is susceptible to EIS, and thus the coupled features of permeability and seam mechanical properties need to be considered in gas transport. The coupling of the desorption contraction as well as adsorption expansion properties of the coal matrix and the geomechanics properties is critical to the interpretation of coal seam permeability (Luke et al., 2010), and the essence of permeability control by EIS is to reduce the permeability through deforming the pore structure of the coal reservoir and reducing the pore fracture volume, thus causing large irreversible damage to the permeability in all directions. The fracture compression coefficient is a parameter that characterizes the dynamic change of permeability with EIS variation and can reflect the stress sensitivity of coal reservoir permeability during CBM development (Chen et al., 2017). The control of permeability direction by EIS is caused by the spatial difference of compression of coal matrix fractures by EIS (Liu et al., 2019).

It is noteworthy that the above scholars’ understanding of permeability and EIS gives priority to the whole process of pressure-reducing extraction in the practice of coalbed methane extraction engineering. The coal reservoir permeability is dynamic, which changes with the reservoir environment variation during the CBM development process. In the depressurization and extraction stage, reservoir permeability and EIS are dynamic and closely related, and thus many scholars concentrate on engineering parameters such as permeability stress sensitivity and permeability injury rate. The EIS data obtained in this study are gained from IFOT, which belong to static and non-reservoir injury type. In undeveloped coal reservoirs, the stresses in all directions are in equilibrium. The permeability of coal will be controlled by the relationship between the coal pore fracture system, the magnitude and the direction of *in situ* stress.

Figure 11 shows the relationship between EIS and permeability in the reservoir in western Guizhou area. The variation of permeability is the same as that in Figure 10, and the EIS gradually increases with increasing depth, with a clear trend of variation. Therefore, the monotonic negative exponential relationship between permeability and EIS derived from previous studies is no longer applicable to the specific geological situation of the study area, and it should be discussed in segments.

Qin and Gao (2012) concluded that there is no definite relationship between permeability and burial depth once the permeability of coal seam test wells is below .05 mD. Additionally, the burial depth and pore pressure are closely related to the *in situ* stress, so for Figure 10, some of the extremely low and small values of permeability can be removed appropriately, and most of the valid data

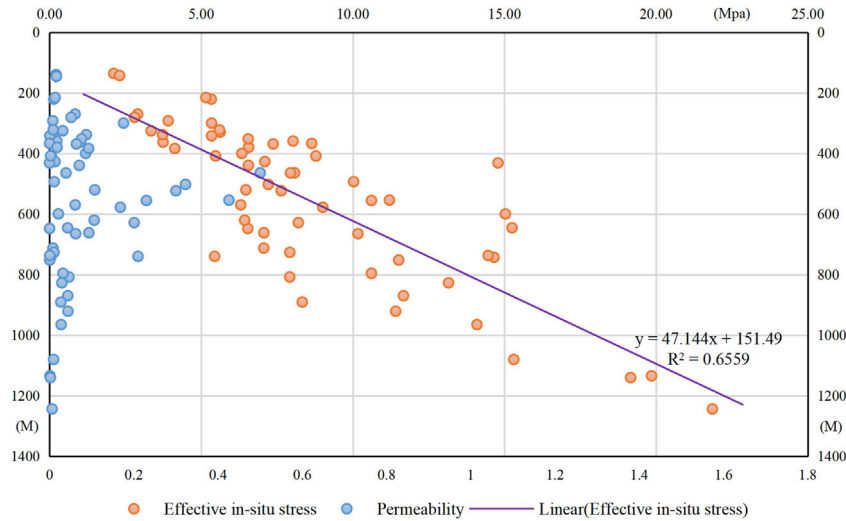


FIGURE 11
Relationship between reservoir EIS and permeability in western Guizhou.

to explore the relationship between reservoir properties can be retained.

Since the monotonic negative exponential relationship between permeability and EIS derived from previous studies is no longer applicable to the study area, this study redefines the control mechanism of EIS on permeability, analyzes the correlation between coal rock permeability and stress, proposes a new coupled calculation model, and performs a least-squares fitting operation.

Let the following power function relationship be satisfied between EIS and permeability data:

$$y = ax^{-b} \tag{20}$$

Take the log of both sides:

$$\ln y = -b \ln x + \ln a \tag{21}$$

Let: $Y = \ln y$, $A = -b$, $X = \ln x$, $B = \ln a$

Convert to linear equation with one variable:

$$Y = AX + B \tag{22}$$

So: $b = -A$, $a = e^B = e^{(Y-AX)}$

Therefore, the problem is transformed into finding the coefficients A and B of a linear equation $Y = AX + B$ with one variable.

The least square method is used to solve the coefficients:

Quadratic loss function $f = \sum_{i=1}^n (y_i - (Ax_i + B))^2$. Where y_i is the true value, $Ax_i + B$ is the fitted value. The objective is to find the coefficients A and B that minimize the function f . Function f calculates partial derivatives of A and B respectively, and let partial derivative = 0.

$$\begin{aligned} \frac{\partial f}{\partial A} &= \sum_{i=1}^n (-2y_i x_i + 2Ax_i^2 + 2x_i B) \\ &= -2(\sum_{i=1}^n x_i y_i - A \sum_{i=1}^n x_i^2 - B \sum_{i=1}^n x_i) = 0 \end{aligned} \tag{23}$$

$$\frac{\partial f}{\partial B} = -2 \sum_{i=1}^n y_i + 2A \sum_{i=1}^n x_i + 2nB = 0 \tag{24}$$

From Eq. 23, $\sum_{i=1}^n x_i y_i - B \sum_{i=1}^n x_i = A \sum_{i=1}^n x_i^2$

$$A = (\sum_{i=1}^n x_i y_i - B \sum_{i=1}^n x_i) / \sum_{i=1}^n x_i^2 \tag{25}$$

Substitute Eq. 25 into Eq. 24 to get:

$$\begin{aligned} \sum_{i=1}^n y_i - \left(\sum_{i=1}^n x_i y_i - B \sum_{i=1}^n x_i \right) \sum_{i=1}^n x_i / \sum_{i=1}^n x_i^2 - nB &= 0 \\ B = \frac{\sum_{i=1}^n y_i - \sum_{i=1}^n x_i y_i \sum_{i=1}^n x_i / \sum_{i=1}^n x_i^2}{\left(n - \sum_{i=1}^n x_i \sum_{i=1}^n x_i / \sum_{i=1}^n x_i^2 \right)} &= \frac{\sum_{i=1}^n y_i \sum_{i=1}^n x_i^2 - \sum_{i=1}^n x_i y_i \sum_{i=1}^n x_i}{n \sum_{i=1}^n x_i^2 - \sum_{i=1}^n x_i \sum_{i=1}^n x_i} \end{aligned} \tag{26}$$

Substituting Eq. 26 into Eq. 25 to get:

$$\begin{aligned} A &= \left(\sum_{i=1}^n x_i y_i - \frac{\sum_{i=1}^n y_i \sum_{i=1}^n x_i^2 - \sum_{i=1}^n x_i y_i \sum_{i=1}^n x_i}{n \sum_{i=1}^n x_i^2 - \sum_{i=1}^n x_i \sum_{i=1}^n x_i} \sum_{i=1}^n x_i \right) / \sum_{i=1}^n x_i^2 \\ &= \frac{n \sum_{i=1}^n x_i y_i - \sum_{i=1}^n x_i \sum_{i=1}^n y_i}{n \sum_{i=1}^n x_i^2 - \sum_{i=1}^n x_i \sum_{i=1}^n x_i} \end{aligned} \tag{27}$$

Substitute EIS and permeability data in this study. In Eq. 22, EIS data is regarded as Y and permeability data is regarded as X.

The result is that when the depth is less than 550 m, $a = 7.771$ and $b = -.07631$ in Eq. 21.

Get formula: $y = 7.771x^{0.07631}$ When the depth is greater than 550 m, $a = 5.85$ and $b = .1865$ in Eq. 21.

Get formula: $y = 5.85x^{-0.1865}$

The final results obtained are shown in Figure 12, and the correlation coefficients of the fitting results are .3 and .6, respectively. the correlation coefficients of data points shallower

than 550 m are lower, similar to the aforementioned case of lower correlation between lateral pressure coefficient and permeability. Some scholars believe that coal rock permeability changes are controlled by the combined negative effect of effective stress and positive effect of coal matrix contraction; the double coupling effect complicates the permeability changes (Fu et al., 2002), and the percolation pattern of coal is related to the skeletal deformation and pore structure changes due to effective stress, and this effect has both positive and negative effects (Cao et al., 2022; Zhang et al., 2022). In addition to the effective stress, the permeability is also controlled and influenced by different factors such as stress sensitivity, fracture compression coefficient, coal sample deformation, pore pressure, and different coal rank together, and the fitting results are better in view of the multiple coupling and complexity of permeability.

Hence, unlike most of the previous studies that focused only on the monotonic negative power exponential relationship between *in situ* stress and permeability in drainage depressurization, the *in situ* stress situation when the subsurface rock formation is in hydrostatic equilibrium is more complex than expected but still has a pattern to follow. The static permeability takes shape through the long-term geological structure, hydrogeology, and coalification of the reservoir, and is the equilibrium of the undeveloped reservoir in a stable geological state for a long time. In Figure 12, the study area displays a single-peaked permeability pattern coupled with a monotonically increasing EIS, and the EIS together with permeability shows distinct characteristics of stages by depth.

The features of western Guizhou vertical permeability change are basically consistent with the location of the stress field transition, indicating that the stress field development law (lateral pressure coefficient, EIS) and the control of the stress field on the reservoir pore and fracture structure jointly affect the permeability of the western Guizhou coal reservoir.

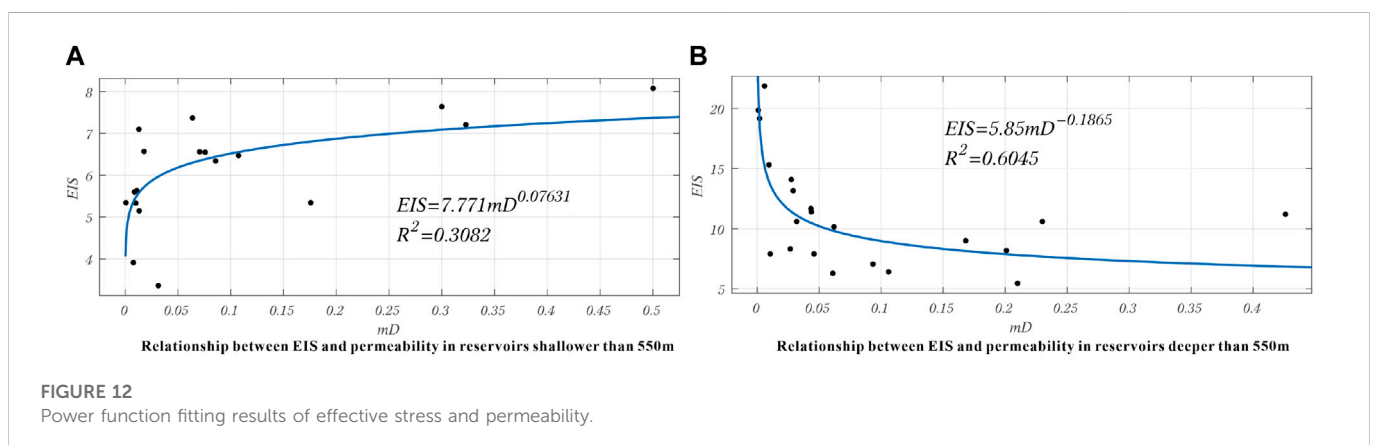
Optimization of CBM development potential

The Upper Permian coal-bearing strata in the study area have typical features of coal seam group development: a multitude of coal seams (5–104 seams), thin single-seam thickness (.6–8.3 m), small seam spacing (5–20 m), large cumulative thickness (6.0–53.5 m), and full distribution of coal species (R_{max} .68%–3.14%), and the resource availability of coal seams varies greatly from region to region (Yang et al., 2011). The characteristics of “One aspect is weak, two aspects are

many, three aspects are high, and four aspects are great” summarized by Gao et al. (2009) are as follows: the Longtan formation, where the coal-bearing strata are located, is low water-abundance, has multiple types of gas-controlling structures and multiple coal seams, possesses high gas content, high resource abundance, high pore pressure and *in situ* stress, and harbours a great many coalbed methane resources, great coal grade variability, great permeability of coal seams and great vertical variation of geological conditions. Due to the special tectonic evolution history of western Guizhou area, the coal seams of the Upper Permian coal-bearing system are mainly preserved in several coal-bearing syncline tectonic units, and the same coal-bearing tectonic units have greater similarity in sedimentary geological background and gas reservoir storage pattern. Hence, this study aims to apply the final classification to each coal-bearing and gas-controlling syncline basin in the selection of coal-bed methane development potential.

Burial depth has the principal influence on both gas content and pore permeability of coal seams, and has a significant impact on the gas production capacity of coal seams, which is one of the primary geological factors to be considered for CBM development. It is generally believed that the gas content of coal seams is positively correlated with the burial depth (Qin and Gao, 2012; Yi et al., 2019; Yang et al., 2020; Gao et al., 2021). The practice in Qinshui basin, China, exhibits that 500–800 m is the ideal burial depth for current CBM development, 800–1,000 m can be exploited, and it is difficult to exploit beyond 1,000 m, and the deeper the burial depth, the higher the cost and the more challenging to achieve economic exploitation (Ji, 2012). Meanwhile, the gas production capacity of coal seam is positively correlated with the reservoir permeability. Concurrently, stress field conversion is momentous for gas production in coalbed methane wells. Stemmed from the previous study, the lateral pressure coefficient k has an extremely strong coupling relationship with the *in situ* stress transformation, and the Z-shaped variation of k value corresponds to the single-peaked trend of permeability variation, and the k value has a strong control on the permeability. Simultaneously, permeability has a strong sensitivity to EIS. The above elements are plotted on the same longitudinal depth map. The relationships of parameters such as triaxial principal stress, EIS, lateral pressure coefficient, and permeability are integrated to determine the boundary depths of the preferred and non-preferred zones. The preferred model of coalbed methane development potential is shown in Figure 13.

Within 400 m, the average EIS value is only 4.89 MPa and the average permeability is .04 mD, which is extremely low. The coal seam



contains low gas content, especially the range within 200 m is the wind oxidation zone of coalbed methane in western Guizhou area, which does not have any value for coalbed methane exploitation. Corresponding to the “Non-preferred area” of the preferred model, in the range of 400–1,000 m, the *in situ* stress is rapidly transformed, and the strike-slip faults and normal faults are dominant, both the parallel to rock strata fractures and the vertical fractures can be greatly expanded and connected, and the lateral pressure coefficient increases first and then decreases, with the average value around 1. EIS continues to increase, with an average value of 9.07 MPa. All the above changes create favorable conditions for the sudden increase of permeability. The gas content of the coal seam increases and the gas production efficiency increases, which corresponds to the “Preferred area” of the preferred model. For coal seam over 1,000 m deep, according to the Chinese geological and mining industry standard (DZ/T 0216-2010), it belongs to the deep coalbed methane. Although the gas content is still increasing, the deep reservoir is characterized by high temperature, high pressure and high *in situ* stress, with extremely low permeability and low gas production efficiency, which corresponds to the “Non-preferred area” of the preferred model.

In 2016, the Yangmei parameters 1 well constructed by China Geological Survey in the Yangmeishu syncline in Liupanshui coalfield and the Wenjiaba 1 well constructed by Guizhou local CBM company in the Zhina coalfield are two famous high-yield wells in Guizhou, with the highest daily gas production of over 5,000 and 6,000 m³ respectively, with high stable gas production and long stable production period. From the perspective of reservoir combination, Yangmei Parameter 1 well is the combination of the upper coal group of Longtan formation, while Wenjiaba 1 well is the combination of the middle and lower coal group of Longtan formation, both containing 3 and 4 layers of coal seam. From the perspective of reservoir properties, the two wells have high gas content, both above 12 m³/t, with high gas saturation. The coal body structure of reservoir combination is good, and all of them are primary-cataclastic structure. It is worth noting that the gas producing reservoir bottom depth of well Yangmei parameter 1 well is 659 m, and the gas producing reservoir bottom depth of Wenjiaba 1 well is 442 m, both of which are within the depth range of “Preferred area” in Figure 13. The average value of the closed pressure gradient of Yangmeishu parameter 1 well is 1.8 MPa/hm, and that of Wenjiaba 1 well is 2.23 MPa/hm. According to the triaxial stress analysis, both wells are in the strike-slip fault stress mode, and the lateral pressure coefficient *k* values are 1.05 and 1.17, respectively. From the analysis of this paper, it can be seen that the lateral pressure coefficient is high, corresponding to the high permeability reservoir. *In situ* permeability indicates that the average permeability of both wells is greater than .1 mD, which corresponds exactly to the conclusions of Figures 10, 13. Although the high yield of CBM wells is also closely related to higher gas content and better coal structure, the coupling relationship between *in situ* stress and permeability, which is concluded in this paper, has been well verified in the actual development and application of CBM.

Further discussion in this thesis puts the accent on issues related to the engineering applications of CBM development. The vertical stress field in western Guizhou area is mainly dominated by normal faults and strike-slip stress fields. Among the normal fault stress fields, vertical boreholes are the most stable type. In contrast, horizontal boreholes drilled along the S_H direction are the most unstable and prone to shear damage and tensor leakage (Ni et al., 2010). In other words, the pipeline

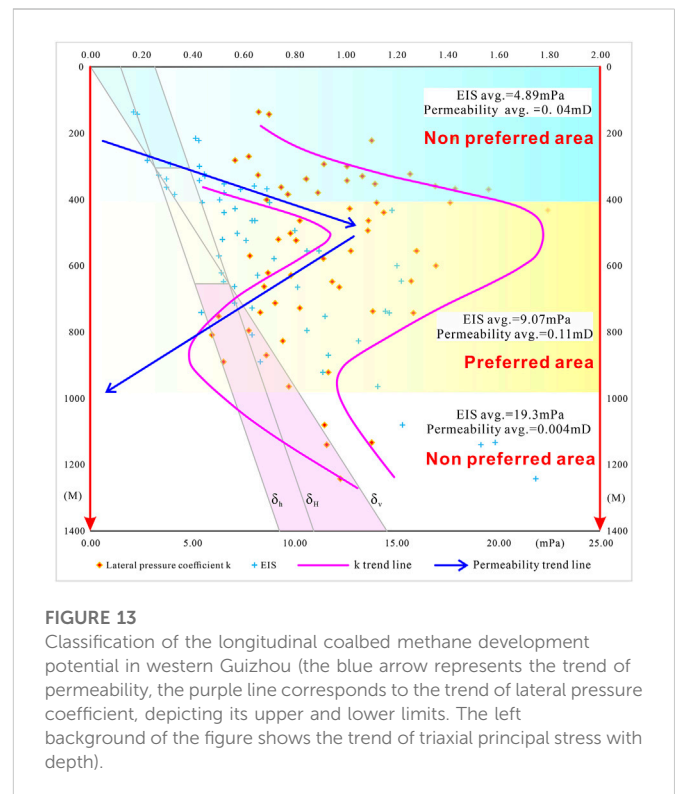


FIGURE 13

Classification of the longitudinal coalbed methane development potential in western Guizhou (the blue arrow represents the trend of permeability, the purple line corresponds to the trend of lateral pressure coefficient, depicting its upper and lower limits. The left background of the figure shows the trend of triaxial principal stress with depth).

is susceptible to damage along the intermediate principal stress direction. Hence, straight (deep) wells should be arranged in the normal fault stress field. And this will generate the problems of pressure reduction difficulties and under-recovery, and single well production is difficult to raise. Learning from the experience of Qinshui and Huainan basins, this problem can be alleviated by placing slave well sets or “Unconventional Gas Reservoir” co-prospecting (Qin et al., 2016). In the strike-slip fault stress field, horizontal boreholes drilled along the S_H direction are the most stable, while vertical boreholes are the least stable and prone to shear damage and tensional leakage (Ni et al., 2010). Consequently, horizontal boreholes along the S_H direction should be deployed in the strike-slip fault stress field.

Conclusion

In this study, the following conclusions are drawn from the study of the coupling relationship between the distribution pattern of the *in situ* stress field and the physical properties of coalbed methane reservoirs in the western Guizhou region of China, as well as the delineation of the vertical development unit of coalbed methane controlled by the *in situ* stress pattern.

- 1) The average gradient of horizontal principal stress in the study area is 2.70 MPa/hm, partly in the medium stress zone and partly in the high and ultra-high stress zones. Overall, δ_v is the least, and δ_H and δ_h dominate roughly equal environments. Vertically, the strike-slip fault mode dominates at 300–600 m, and the normal fault mode dominates at >600 m. From shallow to deep, it shows an obvious developmental feature of reverse fault mode → strike-slip fault mode → normal fault mode.

- 2) The pore pressure P_p , breakdown pressure P_b , and closure pressure P_c increase linearly with depth at different depths and different coal-bearing syncline and are well correlated. By fitting the trend line equation by multiple comparisons, a new simplified model diagram of triaxial principal stress and depth in the study area is proposed.
- 3) Using the [Brown-Hoek \(1978\)](#) method to obtain the lateral pressure coefficient stress ratio k to study the variation pattern of the stress field, the envelope formula and the median formula of the lateral pressure coefficient k in the study area are calculated. The reasons for the differences between the calculated results and the Hoek-Brown envelope formula and the Chinese ground stress envelope formula are also analyzed. In the vertical direction, the k values are discrete in the shallow part and converge in the deep part. Corresponding the magnitude of k values to the three fault properties, the same triaxial *in situ* stress pattern as in conclusion (2) is found. With increasing depth, k gradually converges to .65. Also, the envelope formula for k values can calculate the value domain of *in situ* stress at different depths in the study area.
- 4) The general permeability in the study area is extremely low, increasing and then decreasing in the vertical direction in a single-peaked V. Shallower than 1,000 m, the permeability has a strong positive correlation with the lateral pressure coefficient that varies in a Z-shaped pattern. The zone of rapidly decreasing permeability (600–700 m) also corresponds largely to the stress transition zone from the strike-slip fault mode to the normal fault mode. The control pattern and mechanism of the lateral pressure coefficient k on permeability are discussed. The same pattern of *in situ* stress transition as in conclusion (2) is found.
- 5) The reservoir permeability is highly sensitive to EIS, and the mechanism of EIS control on permeability is deeply analyzed, and a new coupled calculation model is proposed. A new relationship is revealed that is different from the monotonic negative exponential relationship between permeability and EIS considered by previous authors.
- 6) According to the characteristics of burial depth, permeability and gas content, western Guizhou vertical CBM is divided into three development potential areas. 400–1,000 m is the most favorable vertical development area with high gas content, high permeability and moderate burial depth, which is conducive to the development of CBM.

Data availability statement

The original contributions presented in the study are included in the article/Supplementary Material, further inquiries can be directed to the corresponding authors.

References

- Anderson, B. E. M. (1951). The dynamics of faulting. *W.S. Cowell*.
- Bell, J. (2006). *In-situ* stress and coal bed methane potential in Western Canada. *Bull. Can. Petroleum Geol.* 54 (3), 197–220. doi:10.2113/gscpgbull.54.3.197
- Bi, C. (2018). CBM resources and distribution in China. *Pet. Knowl.* (2), 12.
- Biot, M. A. (1962). Theory of propagation of elastic waves in a fluid-saturated porous solid. I. Low-Frequency range. *J. Acoust. Soc. Am.* 28, 168–178. doi:10.1121/1.1908239
- Bodden, W. R., and Ehrlich, R. (1998). Permeability of coals and characteristics of desorption tests: Implications for coalbed methane production. *Int. J. Coal Geol.* 35 (1), 333–347. doi:10.1016/s0166-5162(97)00039-6
- Bredehoeft, J. D., Wolff, R. G., Keys, W. S., and Shuter, E. (1976). Hydraulic fracturing to determine the regional *in situ* stress field, Piceance Basin, Colorado. *GSA Bull.* 87 (2), 250–258. doi:10.1130/0016-7606(1976)87<250:hfdtr>2.0.co;2
- Brown, E. T., and Hoek, E. (1978). Trends in relationships between measured *in-situ*, stresses and depth. *J. Int. J. Rock Mech. Min. Sci. Geomechanics Abstr.* 15 (4), 211–215. doi:10.1016/0148-9062(78)91227-5
- Cao, M., Deng, Z., Kang, Y., Li, Z., Zhang, B., Qing, S., et al. (2022). The dual coupling effect of coal sample permeability effective stress and matrix shrinkage and its relationship with coal rank. *Geol. Rev.* 68 (05), 1863–1870. doi:10.16509/j.georeview.2022.04.011

Author contributions

RDY, TSY, and FL designed the study. WG designed the manuscript. XW optimizes the mathematical methods used in the study. YZ and GL edited the chart. WG, RLL, and ZHY are responsible for data collection and collation. RDY, TSY, WG, and WC put forward some ideas of the article and the interpretation of the data, YHL assisted in the analysis of the data. FL analyzed the data, wrote the manuscript, and translated it. All co-authors reviewed and revised the final version of the manuscript.

Funding

This work was funded by National Natural Science Foundation of China, No. U1812402, Guizhou Provincial Science and Technology Innovation Talent Team Project [QianKeHePingTai No. (2018) 5613], Evaluation of underground coal gasification resources and site selection for pilot trial [QianKeHeZhongDa No. (2021) 3002], Guizhou Science and Technology Program Project: Key Technology and Engineering Test of Coal-bed methane (coal mine gas) Extraction, Production and Efficiency Enhancement in Guizhou Province [No. (2022) ZD001]. All experiments were in compliance with the current laws of the country in which they were performed.

Acknowledgments

The author thanks the technicians of Guizhou Coalfield Geological Bureau for their valuable suggestions.

Conflict of interest

The authors declare that the research was conducted in the absence of any commercial or financial relationships that could be construed as a potential conflict of interest.

The reviewer YH declared a shared affiliation with the authors YL, GL to the handling editor at time of review.

Publisher's note

All claims expressed in this article are solely those of the authors and do not necessarily represent those of their affiliated organizations, or those of the publisher, the editors and the reviewers. Any product that may be evaluated in this article, or claim that may be made by its manufacturer, is not guaranteed or endorsed by the publisher.

- Chen, J., Kang, Y., You, L., and Fang, J., (2011). Research progress and prospect of stress sensitivity of low permeability reservoirs. *Nat. Gas. Geosci.* 22 (1), 182–189.
- Chen, S., Tang, D., Tao, S., Xu, H., Li, S., Zhao, J., et al. (2018). Statistic analysis on macro distribution law of geostress field in coalbed methane reservoir. *Coal Sci. Technol.* 46 (6), 57–63. doi:10.13199/j.cnki.cst.2018.06.010
- Chen, S., Tang, D., Tao, S., Xu, H., Li, S., and Zhao, J., (2017). *In-situ* stress measurements and stress distribution characteristics of coal reservoirs in major coalfields in China: Implication for coalbed methane (CBM) development. *Int. J. Coal Geol.* 182, 66–84. doi:10.1016/j.coal.2017.09.009
- Chen, X. (2009). *Probability theory and mathematical statistics*. Hefei, China: China University of Science and Technology Press.
- Cheng, W., Yang, R., and Zhang, Q., (2015). *Distribution characteristics, enrichment law and clean potential of trace elements in late Permian coal in Liupanshui coalfield: Distribution characteristics, enrichment law and clean potential of trace elements in late Permian coal in Liupanshui coalfield*. Guizhou Science and Technology Press. Guiyang, China.
- Dou, X., Jiang, B., Qin, Y., Wang, W., and Chen, W., (2012). Tectonic evolution and its control over late Permian coal seams in Western Guizhou. *Coal Sci. Technol.* 40 (3), 109–114. doi:10.13199/j.cst.2012.03.114.douxzh.002
- Enever, J., and Henning, A. (1997). *International coalbed methane symposium*. : The University of Alabama Tuscaloosa, Tuscaloosa, AL, USA 13–22. The relationship between permeability and effective stress for Australian coal and its implications with respect to coalbed methane exploration and reservoir modeling
- Engelder, T. (1993). *Stress regimes in the lithosphere*. Princeton, NJ, USA: Princeton University Press.
- Fu, X., Li, D., Qin, Y., Jiang, B., Wang, W., Li, G., et al. (2002). Experimental research of influence of coal matrix shrinkage on permeability. *J. China Univ. Min. Technol.* 31 (2), 129–137.
- Fu, X., Qin, Y., and Wei, C. (2007). *Coalbed methane geology*. Xuzhou, China: China University of Mining and Technology Press.
- Gao, D., Qin, Y., and Yi, T. (2009). On the geological characteristics and exploration and development strategy of coalbed methane in Guizhou. *China coal Geol.* 21 (3), 20–23.
- Gao, W., Han, Z., Jin, J., Bai, L., and Zhou, P., (2018). Occurrence characteristics and favorable area evaluation of coalbed methane in Liupanshui coalfield. *Coalf. Geol. Explor.* 46 (5), 81–89. doi:10.3969/j.issn.1001-1986.2018.05.013
- Gao, W., Han, Z., Bai, L., and Jin, J., (2021). Geological characteristics and differential causes of coal seam gas bearing in Liupanshui area, 25, 1–10. *Coal Sci. Technol.*
- Griffith, A. A. (1920). The phenomena of rupture and flow in solids. *Philosophical Trans. R. Soc. A Math. Phys. Eng. Sci.* A221 (4), 163–198.
- Guo, M. (2012). *Study on permeability law of high-rank coal reservoirs under effective stress*. Beijing, China: China University of Petroleum.
- Haimson, B. C., and Cornet, F. H. (2003). ISRM suggested methods for rock stress estimation-part 3: Hydraulic fracturing (HF) and/or hydraulic testing of pre-existing fractures (HTPF). *Int. J. Rock Mech. Min. Sci.* 40 (7-8), 1011–1020. doi:10.1016/j.ijrmm.2003.08.002
- Han, J., Zhang, H., Li, S., and Song, W. (2012). The characteristic of *in situ* stress in outburst area of China. *Saf. Sci.* 50 (4), 878–884. doi:10.1016/j.ssci.2011.08.014
- Hillis, R. R., Enever, J. R., and Reynolds, S. D. (1999). *In situ* stress field of eastern Australia. *J. Geol. Soc. Aust.* 46 (5), 813–825. doi:10.1046/j.1440-0952.1999.00746.x
- Hoek, E., and Brown, E. T. (1980). *Underground excavations in rock*. The Institute of Mining and Metallurgy London, UK.
- Hu, Q., Li, M., Qiao, M., Liu, C., Liu, S., Fan, B., et al. (2017). Analysis on key geological factors of fracturing effect of high-order coal-bed gas wells in the south of Qinshui Basin. *J. China Coal Soc.* 42 (6), 1506–1516. doi:10.13225/j.cnki.jccs.2016.1161
- Jasinge, D., Ranjith, P., and Choi, S. (2011). Effects of effective stress changes on permeability of latrobe valley Brown coal. *Fuel* 90 (3), 1292–1300. doi:10.1016/j.fuel.2010.10.053
- Ji, M. (2012). Evaluation of favorable blocks for surface drainage of CBM in Gaohe coal mine, Lu'an coalfield. *Coal Geol. Explor.* 40 (3), 36–39. doi:10.3969/j.issn.1001-1986.2012.03.009
- Jin, J., Yang, Z., Qin, Y., Cui, Y., Wang, G., Yi, T., et al. (2021). Development progress, potential and Prospect of coalbed methane in Guizhou Province. *J. China Coal Soc.*, 1–13.
- Jing, F., Sheng, Q., Zhang, Y. H., and Liu, Y. K. (2008). Statistical analysis of the distribution law of ground stress in rocks of different geological genesis. *Geotechnical Mechanics*, 8 1877–1883. doi:10.16285/j.rsm.2008.07.0357
- Kang, H., Jiang, T., Zhang, X., and Yan, L., (2009). Research and application of *in-situ* stress field in jincheng mining area. *J. rock Mech. Eng.* 28 (1), 8.
- Kang, H., Zhang, X., Si, L., Wu, Y., and Gao, F. (2010). *In-situ* stress measurements and stress distribution characteristics in underground coal mines in China. *Eng. Geol.* 116, 333–345. doi:10.1016/j.enggeo.2010.09.015
- Karacan, C., Ulery, J., and Goodman, G. (2008). A numerical evaluation on the effects of impermeable faults on degasification efficiency and methane emissions during underground coal mining. *Int. J. Coal Geol.* 75 (4), 195–203. doi:10.1016/j.coal.2008.06.006
- Li, Y., Tang, D., Xu, H., Meng, Y., and Li, J. (2014). Experimental research on coal permeability: The roles of effective stress and gas slip-page. *J. Nat. Gas Sci. Eng.* 21, 481–488. doi:10.1016/j.jngse.2014.09.004
- Liu, D., Zhou, S., Cai, Y., and Yao, Y., (2017). Study on effect of geo-stress on coal permeability and its controlling mechanism. *Coal Sci. Technol.* 45 (6), 1–823. doi:10.13199/j.cnki.cst.2017.06.001
- Liu, S., and Harpalani, S. (2013). Permeability prediction of coalbed methane reservoirs during primary depletion. *Int. J. Coal Geol.* 113 (3), 1–10. doi:10.1016/j.coal.2013.03.010
- Liu, S., Yang, Z., Zhang, Z., and Cao, T., (2019). Study on the differences of effective stress on coal reservoirs permeability in different directions. *Nat. Gas. Geosci.* 30 (10), 1422–1429.
- Liu, X., Luo, P., and Meng, Y. (2004). Study on the influence of *in-situ* stress field on wellbore trajectory design and stability. *Nat. Gas. Ind.* (09), 57–59.
- Lu, Z., Tao, M., Li, Q., Wu, P., Gu, S., Gao, W., et al. (2022). Gas geochemistry and hydrochemical analysis of CBM origin and accumulation in the Tucheng syncline in western Guizhou Province. *Geochem. J.* 56 (2), GJ22005. doi:10.2343/geochem.GJ22005
- Luke, D. C., Lu, M., and Pan, Z. J. (2010). An analytical coal permeability model for tri-axial strain and stress conditions. *Int. J. Coal Geol.* 84, 103–114. doi:10.1016/j.coal.2010.08.011
- Lv, F., Yang, R., Yi, T., and Gao, W., (2021). A prediction model of coal structure based on logging parameters in Liupanshui Coalfield, Guizhou, China. *Arabian J. Geosciences* 14, 2204. doi:10.1007/s12517-021-08519-9
- McKee, C. R., Bumb, A. C., and Koenig, R. A. (1988). Stress dependent permeability and porosity of coal and other geologic formations. *SPE Form. Eval.* 3, 81–91. doi:10.2118/12858-PA
- Men, X., Tao, S., Liu, Z., Tian, W., and Chen, S. (2021). Experimental study on gas mass transfer process in a heterogeneous coal reservoir. *Fuel Process. Technol.* 216, 106779. doi:10.1016/j.fuproc.2021.106779
- Meng, Z., Tian, Y., and Li, G. (2010). Characteristics of *in-situ* stress field in Southern Qinshui Basin and its research significance. *J. China Coal Soc.* 35 (6), 975–981. doi:10.13225/j.cnki.jccs.2010.06.014
- Meng, Z., Zhang, J., and Wang, R. (2011). *In-situ* stress, pore pressure and stress-dependent permeability in the Southern Qinshui Basin. *Int. J. Rock Mech. Min. Sci.* 48 (1), 122–131. doi:10.1016/j.ijrmm.2010.10.003
- Ni, X., Su, X., and Zhang, X. (2010). *Geology of coalbed methane development*. Beijing, China: Chemical Industry Press.
- Nur, A., and Byerlee, J. D. (1971). An exact effective stress law for elastic deformation of rock with fluids. *J. Geophys. Res.* 76 (26), 6414–6419. doi:10.1029/jb076i026p06414
- Palmer, I., and Mansoori, J. (1998). How permeability depends on stress and pore pressure in coalbeds: a new model, 12. *Society of Petroleum Engineers*, 539–544. doi:10.2118/36737-MS
- Pan, Z., and Luke, D. (2017). *Characterization and modeling of coalbed methane permeability*. Xuzhou, China: China University of Mining and Technology Press.
- Pashin, J. C. (2007). Hydrodynamics of coalbed methane reservoirs in the black Warrior basin: Key to understanding reservoir performance and environmental issues. *Appl. Geochem.* 22 (10), 2257–2272. doi:10.1016/j.apgeochem.2007.04.009
- Pashin, J. C. (1998). Stratigraphy and structure of coalbed methane reservoirs in the United States: An overview. *Int. J. Coal Geol.* 35 (1/4), 209–240. doi:10.1016/s0166-5162(97)00013-x
- Qi, X., and Dong, S. (2017). *Seismic attribute response of coalbed methane reservoir*. China University of Mining and Technology Press. Xuzhou, China
- Qin, Y., and Gao, D. (2012). *Prediction and evaluation of coalbed methane resource potential in Guizhou Province*. China University of Mining and Technology Press. Xuzhou, China
- Qin, Y., Shen, J., and Shen, Y. (2016). Joint mining compatibility of superposed gas-bearing systems: A general geological problem for extraction of three natural gases and deep CBM in coal series. *J. China Coal Soc.* 41 (1), 14–23. doi:10.13225/j.cnki.jccs.2015.9032
- Qin, Y., Zhang, D., Fu, X., Lin, D., Ye, J., and Xu, Z., (1999). A discussion on correlation of modern tectonic stress field to physical properties of coal reservoirs in central and southern Qinshui Basin. *Geol. Rev.* 45 (6), 576–583.
- Salmachi, A., Rajabi, M., Wainman, C., Mackie, S., McCabe, P., and Camac, B., (2021). History, geology, *in situ* stress pattern, gas content and permeability of coal seam gas basins in Australia: A review. *Energies* 14 (2651), 2651. doi:10.3390/en14092651
- Sang, S., Han, S., Liu, S., Zhou, X., Li, M., Hu, Q., et al. (2022). Comprehensive study on the enrichment mechanism of coalbed methane in high rank coal reservoirs. *J. China Coal Soc.* 47 (1), 388–403. doi:10.13225/j.cnki.jccs.yg21.1854
- Shi, J. Q., and Durucan, S. (2005). A model for changes in coalbed permeability during primary and enhanced methane recovery. *SPE Reserv. Eval. Eng.* 8 (4), 291–299. doi:10.2118/87230-PA
- Sun, L., Kang, Y., Wang, J., Jiang, S., Zhang, B., Gu, J., et al. (2017). Vertical transformation of *in-situ* stress types and its control on coalbed reservoir permeability. *Geol. J. China Univ.* 23 (1), 148–156. doi:10.16108/j.issn1006-7493.2016156

- Tang, S., Zhu, B., and Yan, Z. (2011). Effect of crustal stress on hydraulic fracturing in coalbed methane wells. *J. China Coal Soc.* 36 (1), 65–69. doi:10.13225/j.cnki.jccs.2011.01.005
- Tang, X. (2012). Occurrence law of coal resources in Guizhou Province. *Coalf. Geol. Explor.* 40 (5), 1–5.
- Tavener, E., Flottmann, T., and Brooke, B. S. (2017). 458. Geological Society London Special Publications, 31–47. doi:10.1144/SP458*in situ stress distribution Mech. Stratigr. Bowen Surat basins, queensland, Australia*
- Terzaghi, K. V. (1923). Die Berechnung der Durchlässigkeit des Tonen aus dem Verlauf der hydrodynamischen Spannungserscheinungen. *Sitzungsber. Akad. Wiss. Math. Naturwiss. Kl. Abt.132*
- Vishal, V., Ranjith, P. G., Pradhan, S. P., and Singh, T. N. (2013). Permeability of sub critical carbon dioxide in naturally fractured Indian bituminous coal at a range of down-hole stress conditions. *Eng. Geol.* 167, 148–156. doi:10.1016/j.enggeo.2013.10.007
- Wang, J., Qin, Y., and Zhu, X. (2012). Dynamic changes laws of the coal reservoirs permeability under the superimposition of multi influential factors. *J. China Coal Soc.* 37 (8), 1348–1353. doi:10.13225/j.cnki.jccs.2012.08.013
- Wang, X., Zhao, J., Zhang, Z., and Li, H., (2019). Characteristics of *in-situ* stress development and its control on coal reservoir pressure and permeability in northeastern Pingdingshan Mining area. *Coal Eng.* (6), 6–10.
- Wu, S., Tang, D., Li, S., Wu, H., Hu, X., and Zhu, X. (2017). Effects of geological pressure and temperature on permeability behaviors of middle-low volatile bituminous coals in eastern Ordos Basin, China. *J. Petroleum Sci. Eng.* 153, 372–384. doi:10.1016/j.petrol.2017.03.034
- Xu, H. J., Sang, S., and Yang, J. (2021). *Development technology evaluation of coalbed methane for multi-coal seam zones in western Guizhou*. Guizhou, China, University of Science and Technology of China Press.
- Xu, H., Sang, S., Yang, J., Jin, J., Hu, Y., Liu, H., et al. (2016). *In-situ* stress measurements by hydraulic fracturing and its implication on coalbed methane development in Western Guizhou, SW China. *J. Unconv. Oil Gas Resour.* 15, 1–10. doi:10.1016/j.juogr.2016.04.001
- Xue, P., Zheng, P., Xu, W., Ren, X., Huang, C., and Du, J., (2015). Influence of effective stress on permeability of different rank coals. *Sci. Technol. Rev.* 33 (2), 69–73. doi:10.3981/j.issn.1000-7857.2015.02.010
- Yang, Z., Qin, Y., and Gao, D. (2011). Coalbed Methane (CBM) reservoir-forming character under conditions of coal seam groups. *Coal Geol. Explor.* 39 (05), 22–26. doi:10.3969/j.issn.1001-1986.2011.05.006
- Yang, Z., Qin, Y., Li, Y., Sun, H., and Yi, T. (2020). *Geological evaluation technology of coalbed methane multi-layer combined mining development*. Xuzhou, China: China University of Mining and Technology Press.
- Yi, T. (1997). Occurrence characteristics of coalbed methane in Guizhou Province. *Guizhou Geol.* (4), 346–348.
- Yi, T., Sang, S., and Jing, J. (2019). *Key technology and engineering application of surface extraction of coalbed methane in Guizhou Province*. Xuzhou, China: China University of Mining and Technology Press.
- Yin, G., Li, W., Li, M., Li, X., Deng, B., and Jiang, C., (2014). Permeability properties and effective stress of raw coal under loading-unloading conditions. *J. China Coal Soc.* 39 (8), 1497–1503. doi:10.13225/j.cnki.jccs.2014.9011
- Yuan, Z. (2004). Research on mechanism of tectonic stress field controlling coal permeability. *Coal Geol. Explor.* 32 (4), 23–25.
- Zhang, T., Meng, Y., Pang, M., Zhang, L., and Wu, J., (2022). The effect of effective stress on the evolution of permeability patterns in perforated fractured coal bodies. *Coal Sci. Technol.*, 1–10. doi:10.13199/j.cnki.cst.2022-1349
- Zhao, D. A., Chen, Z. M., Cai, X., and Li, S., (2007). Analysis of distribution rule of geostress in China. *J. Rock Mech. Eng.* 26 (6), 1265–1271. doi:10.3321/j.issn:1000-6915.2007.06.024
- Zhao, J. L., Tang, D. Z., Lin, W., Qin, Y., and Xu, H. (2019). *In-situ* stress distribution and its influence on the coal reservoir permeability in the Hancheng area, eastern margin of the Ordos Basin, China. *J. Nat. Gas Sci. Eng.* 61, 119–132. doi:10.1016/j.jngse.2018.09.002
- Zhou, J., Xian, X., Jiang, Y., Li, X., and Jiang, D., (2009). A permeability model including effective stress and coal matrix shrinking effect. *J. Southwest Petroleum Univ. Sci. Technol. Ed.* 31 (1), 4–8.
- Zhu, H., and Tao, Z. (1994). State of *in-situ* stress in different rocks. *Acta Seismol. Sin.* 7 (1), 67–83. doi:10.1007/bf02651911
- Zhu, P. (2018). *The tectonic evolution and its effect on mine structure of Panguan syncline*. Xuzhou: China University of Mining and Technology. Xuzhou, China
- Zoback, M. D., Barton, C. A., Brudy, M., Castillo, D., Finkbeiner, T., and Grollmund, B., (2003). Determination of stress orientation and magnitude in deep wells. *Int. J. Rock Mech. Min. Sci.* 40 (7-8), 1049–1076. doi:10.1016/j.ijrmms.2003.07.001

Glossary

List of symbols

CBM Coalbed methane

P_b Breakdown pressure

δ_{Hmax} (**δ_H**) Maximum horizontal principal stress

P_c Closure pressure

δ_{Hmin} (**δ_h**) Minimum horizontal principal stress

P_p Pore pressure

δ_v Vertical stress

T_o Tensile strength

EIS Effective *in-situ* stress

P_h Liquid head

P Permeability

H Burial depth

IFOT Injection/fall-off test

k Lateral pressure coefficient